

Nanocellulose and Its Interface: On the Road to the Design of Emerging Materials

Paolo Bettotti and Marina Scarpa*

Nanocellulose has several unique properties that render it a versatile material with possible uses in a broad spectrum of applications. Nanocellulose is proved to form stable colloidal suspensions with interesting rheological properties, assemble in soft hydrogels of tunable porosity, compact dried films. Suggested or already current applications of these systems are in the field of electronics, biomedical, textile, and printing technologies. This review reports on the recent and emerging trends in nanocellulose research concerning the behavior, design, and modification of its interface. This nanomaterial is obtained by a biological source and its behavior is dictated from the composition and structure of native cellulose. The understanding of interface phenomena and their manipulation are the main issues for the effective manufacture of emulsions, coatings and films. In reviewing the recent applications, emphasis is placed on the systems which require control of the order and dynamic of nanocellulose assembly to realize smart materials exploiting the rich and complex behavior of nanocellulose.

1. Introduction

Nature is often the best possible source of inspiration to create functional materials for specific applications: the evolution of natural systems is an effective process to select among the possible technical solution and nature provides a plethora of examples of complex assembled structures based on hierarchical architectures affording specific functionalities. Wood and cellulose structures are striking examples of complex bio-architectures designed to fulfill specific functional requirements: different lengths of building blocks, arranged to provide a broad spectrum of functions, covering from microscopic (e.g., cell walls, elastic and rigid fibers) to macroscopic (e.g., pine and wheat awn actuators^[1]) length scales.

P. Bettotti, M. Scarpa
Nanoscience Laboratory
Department of Physics
University of Trento
via Sommarive 14, Povo, Trento 38123, Italy
E-mail: marina.scarpa@unitn.it

The ORCID identification number(s) for the author(s) of this article can be found under <https://doi.org/10.1002/admi.202101593>.

© 2021 The Authors. Advanced Materials Interfaces published by Wiley-VCH GmbH. This is an open access article under the terms of the Creative Commons Attribution-NonCommercial License, which permits use, distribution and reproduction in any medium, provided the original work is properly cited and is not used for commercial purposes.

DOI: 10.1002/admi.202101593

The interest in the hierarchical structure, the multi-scale organization, and the properties of cellulose has long been the prerogative of botanists and plant physiologists. The last decade has witnessed the potential of a top-down approach to take apart cellulose-based raw materials into their micro- and nano-sized building blocks and to use them to design and fabricate functional materials and devices with new and, in some cases, outstanding properties. At present, cellulose is not only one of the main constituents of the plant and bacterial kingdom, it is also an important component of materials and manufactured goods, such as paper, textiles, or food additives. Depending on the extent of the scale down process, the fragments have variable size and in this review are collectively indicated as nanocellulose (NC).

Although the interfacial properties of NC are always mentioned and recognized to contribute significantly to NC behavior, there is still room for reviewing the several recent reports highlighting the role of the interaction at the interface. In this scenario, the interface driven performances of some advanced NC-based materials are gaining in importance. This review aims at providing an overview of the most advanced of them, such as the Pickering emulsions, the supercapacitors, the drug crystallizing capsules, the nanowood.

In nature, cellulose is synthesized by plants and also by some bacterial strains which can polymerize the glucose residues into linear β -1, 4-glucan chains. Once extracellularly secreted, the chains assemble, crystallize (the degree of crystallinity is up to 90%), and form nanostructures called bacterial nanocellulose (BNC) which in turn assemble forming microfibrils. Different from plant tissues where cellulose is embedded in a heterogeneous macrostructure, bacterial secretions are made of pure cellulose and are considered an excellent source of NC.^[2] However, due to the large availability of cellulose from wood or other low-cost vegetable sources such as agriculture wastes, plant cellulose is the most common material for NC production. Several strategies for the preparation of NC have been reported.^[3] A popular production route uses a pretreatment to introduce negative charges by 2,2,6,6-tetramethylpiperidine-1-oxyl (TEMPO) mediated oxidation followed by a mechanical disintegration.^[4] The behavior of NC has been largely studied, and it is well assessed that when NC colloidal suspensions are dried, they form flexible and transparent films with multifunctional properties.^[5] These properties, first of all, depend on the degree of fibrillation of the colloidal NC.^[6] Conversely, in aqueous solutions, NC

entanglements and form gel networks.^[7] NC is a multifaceted material and several peculiar characteristics and applications have been reviewed: from the fundamentals behind the hierarchical organization,^[8] the key advances in chemical modification,^[9] the surface engineering,^[10] the removal of the barriers to successful NC commercialization such as dewatering-drying process,^[11] and finally, the plethora of the NC applications, in particular the biomedical and bio mimicking applications^[12] and printed electronics.^[13] This literature has motivated a remarkable number of review articles, some of which are cited in the next sections. Herein, we focus on the fundamental aspects of the interfacial properties of NC and how they govern both the fabrication and the application of NC-derived materials and devices. Indeed, NC is not a molecule; it is a nanostructure with peculiar characteristics established by biological evolution, and only partially modifiable by chemical and physical processes. In particular, we will focus on the role of hydroxyls and their hydrogen bonds which contribute to NC stabilization, drive the interaction with water, and provide sites for chemical modification and interfacial interactions. The crucial role of this network for the cellulose structure has long been known; however, at present, the focus is on its dynamics in the bulk and at the interphase when cellulose is scaled down to the nano size. The understanding of these mechanisms helps in the development of technologies to control them and provides the basis for the design of the NC functional materials of the future.

The review is organized as follows: Section 2 describes the structure of NC and the complex interactions between the amphiphilic NC and aqueous environment. Section 3 deals with the interface effects which contribute to the random or ordered arrangement of NC in the dried state and on the techniques by which we can tune these effects to obtain the desired properties. Section 4 reports on the NC reactivity and surface modifications which are instrumental to Section 5 that deals with surface mediated phenomena currently on the limelight for emerging applications such as: the crystallization process induced by NC, the use NC as Pickering emulsifier, and the piezo-triboelectric effect. Moreover Section 5 reports also a very innovative approach to obtain ordered cellulose nanostructures without disrupting the original wood architecture (the so called nano-wood).

2. Structure of the Cellulose and the Role of Hydroxyls

2.1. The Structure of the Cellulose

Despite the chemical simplicity of cellulose, its structure is rather complex and multiscale organized. Cellulose is made of elementary crystalline elements, alternating with regions of less order, organized in fibrils.^[14] In plants, cellulose forms hierarchical supramolecular assemblies where bundles of fibrils interact with hemicellulose and lignin as shown in **Figure 1**. Hydroxyls contribute to this hierarchical organization, since a network of hydrogen bonds works as a glue, providing stiffness and other tissue properties. In fact, cellulose is composed of unbranched glucan chains where the monomers are linked together by β -1, 4-glycosidic bonds and the internal ones contain three free hydroxyls (**Figure 1a**) that give rise to a strong network of hydrogen bonds.

Cellulose is known to have six different polymorphs^[15,16] all sharing a similar structure in which cellobiose chains are packed into either monoclinic or triclinic crystals. The structure of the most common polymorph is well known, while some questions remain about the less studied forms and on their transformation between the different forms (a recent review of the history of the crystallographic studies on cellulose is ref. [17]). **Figure 2** is the sketch of the known polymorphs and how they can be transformed one into the other by proper physico-chemical treatments (more detailed discussions can be found in focused publications such as ref. [18]).

Because of their different structure, different polymorphs show variable mechanical properties. Since the I_β form is the one commonly produced by plants, the vast majority of the reports focus on this polymorph. A rather complete resume of both experimental and modeling data spanning over several allomorphs is reported in ref. [19] while a more recent publication describing molecular dynamics modeling of NC polymorphs is ref. [20]. Moreover, it is expected that NC crystalline domains show anisotropic physical properties, coherently with their low crystalline symmetry.^[21,22] Typically, cellulose I shows greater elastic moduli but type II often produces mechanically stronger materials, probably thanks to the denser intersheet hydrogen bond network that forms in this material at the macroscopic scale.^[23,24]

NC possesses an amphiphilic structure since different crystalline faces exposed have largely different polarity^[25–27] as depicted in **Figure 3**. The polarity of the exposed crystal planes depends also on the cellulose polymorph considered: hydrophilic planes are the (100) for cellulose- I_α , the ($\bar{1}10$) and (110) for cellulose- I_β , and ($\bar{1}10$) for regenerated cellulose-II. On the other hand, the (220) planes of cellulose- I_α and of regenerated cellulose-II, and the (200) planes of cellulose- I_β are mostly hydrophobic.^[28]

The role of both sources of cellulose and pretreatments for efficient conversion to NC has been recently reviewed,^[31] in particular, semicrystalline fibril bundles with average lengths of >500 nm, individually dispersible in water, containing intercalated disordered domains or defects called cellulose nanofibrils (CNF),^[32] while crystalline rods with 3–20 nm widths and lengths of <300 nm called cellulose nanocrystals (CNC) can be obtained depending on the plant sources and on the procedures used for cellulose disaggregation. Typical AFM images of CNF (left panel) and CNCs (right panel) are shown in **Figure 4**. The TEMPO mediated oxidation^[4,33] was applied to obtain both the NCs morphologies; however, the chemical and mechanical procedures were made more exhaustive to obtain the CNCs. Since the mechanical properties of bulk nanocellulose materials are different from those of the corresponding basic crystalline domains, and considering the difficulty of performing experiments with properly arranged CNC/CNF, important information are obtained from studies of molecular dynamics that describe the mechanical properties of CNCs assemblies. For example in ref. [34], the authors describe the pivotal role of hydrogen bonds in determining the frictional properties of cellulose nanocrystals and the behavior of stick-slip and stiffness recovery after irreversible deformation; in ref. [35], the authors discuss the increase in both interfacial stiffness and toughness for cellulose nanocrystals interacting via a water-mediated interface for relative humidity comprising between 30% and 50%. Also, in this case, the increased mechanical properties

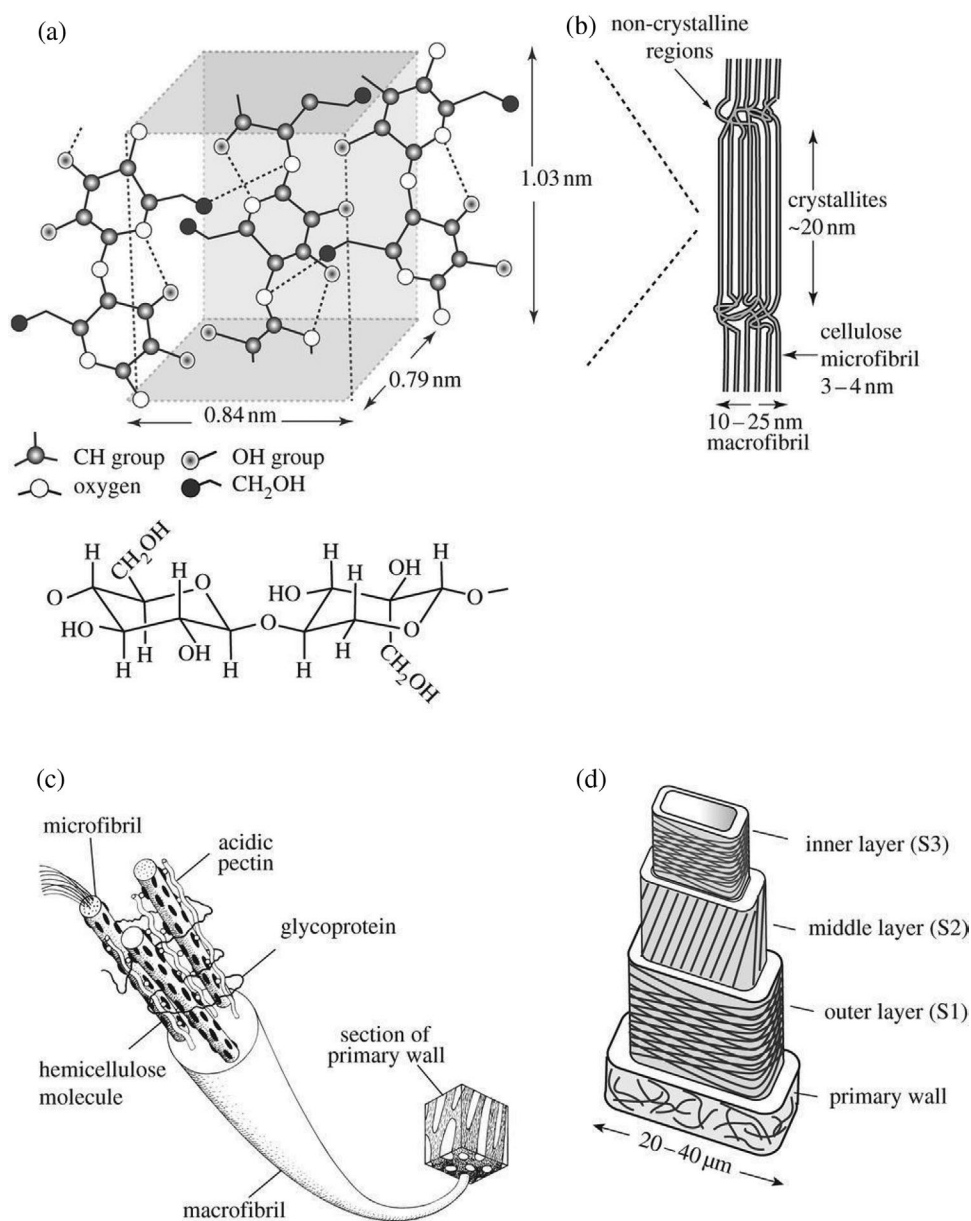


Figure 1. The hierarchical structure of plant cell walls showing: a) the molecular structure of cellulose, with cellobiose molecules (solid line, covalent bonds; dashed line, hydrogen bonds); b) cellulose microfibrils, with both crystalline and non-crystalline regions, aggregated into a macrofibril; c) a macrofibril from a primary cell wall; and d) the cell wall of wood, made up of a primary layer and three secondary layers (S1, S2, and S3), with the cellulose microfibrils arranged in different orientations in each layer. Reproduced with permission.^[14] Copyright 2012, The Royal Society.

are mediated by the formation of a dense hydrogen bond network. Modeling of larger scale domains requires coarse-grain approaches that relieve the computational requirements and some examples were recently proposed.^[36,37]

2.2. The Complex Role of Hydroxyls: The Love–Hate Relationship Between Nanocellulose and Water

Hydrogen bonding, electrostatic, and London dispersion interactions govern the cohesiveness of NC and its dispersion in solvents. Although the contributions of these fundamental

interactions to the overall NC properties is qualitatively well known, a quantitative evaluation is a matter of lively debate. The NC hydroxyl groups are notably excellent hydrogen bond formers and contribute to the irreversible agglomeration during drying and aggregation in non-polar matrices because of the formation of additional hydrogen bonds between nanoparticles.^[3] If the stacking of the hexopyranose rings contributes to the alignment of the glucan chains, the pattern of hydrogen bonds between the hydroxyl groups prompts the highly ordered and stable conformation of the cellulose chains in elementary fibrils,^[38] and the continuous covalent bonding along the nanofibrils provides stiffness and strength.^[39] The so

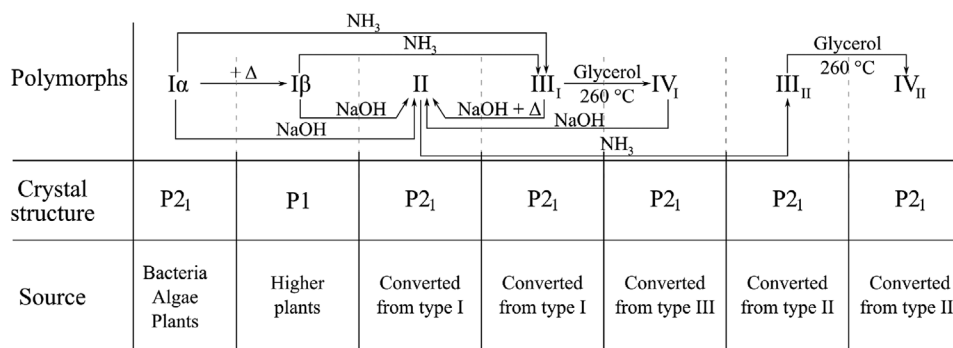


Figure 2. The first line indicates the transformations between cellulose polymorphs. The middle line indicates the crystalline structure of the phases and the bottom one the polymorphs main sources.

resulting structure should be characterized by a high cohesive energy, since NCs remain most entirely intact for years in water solutions in the absence of bacterial or mold contaminations. An approximate but more quantitative idea of the contribution of hydrogen bonding and the dispersion interaction on the cohesive energy of NC was obtained combining experimental enthalpies of sublimation and molecular modeling. These data suggest that, different from small sugars, the London dispersion force provides the main contribution to intermolecular cohesion of cellulose chains in the fibrils, which explains the solvent resistance, and the negligible swelling of cellulose in solvent containing OH and CH groups, such as methanol or ethanol.^[40] The relationship between solubility data and the exposed crystalline surface of wood-based H_2SO_4 -hydrolyzed CNCs was suggested on the bases of the Hansen solubility parameters (HSP: δ_D ; δ_P ; δ_H) measured from sedimentation tests in a wide set of 59 solvents and binary mixtures. Two sets of cohesion parameters corresponding to a polar surface $(18.1; 20.4; 15.3) \pm (0.5; 0.5; 0.4) \text{ MPa}^{1/2}$ and to mildly nonpolar one $(17.4; 4.8; 6.5) \pm (0.3; 0.5; 0.6) \text{ MPa}^{1/2}$ correspond to the (110) and

($\bar{1}\bar{1}0$) surfaces of cellulose $I\beta$ nanocrystals and to the exposure of (200) surfaces.^[41] Indeed, the hydroxyls favor the dispersion of NC in polar media and contribute to the formation of the various phases of NC suspensions, that is, the liquid, gel, and soft glass phases, and confine the water molecules on the (110) and (010) faces of the cellulose crystal,^[42] which affect the dewatering and drying processes. The water affinity of CNCs is proved also by the considerable amount of water absorbed by dry CNCs resulting in a change in thickness of 2 nm.^[43] The hydroxyl bound water, which according to the classification of water in wet pulps is referred to as nonfreezing bound water, and is experimentally detectable since it remains without transition during differential scanning calorimetry freezing and melting cycles. The other two components of water in NC suspensions are the freezing bound water which has a depressed melting temperature because of certain interactions with cellulose, and the excess of water, namely free water, with the properties of bulk water.^[44] NC dispersed in water can entangle and forms gels of variable strength, depending on the NC morphology (CNF are better gel formers than CNC), and on the presence of

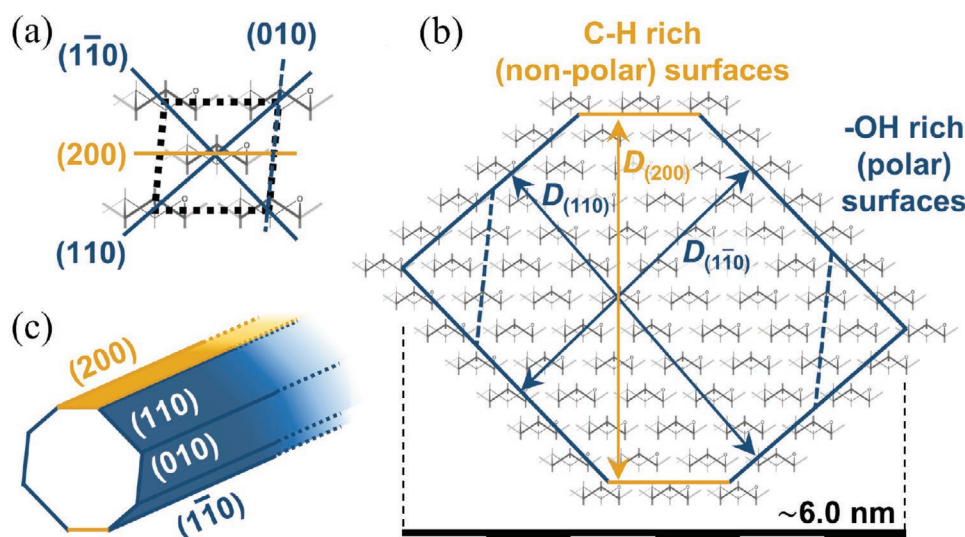


Figure 3. Schematic view of NC crystalline structure. a) P21 unitary cell. The five cellobiose chains are depicted in gray. Hydrophilic (blue) and hydrophobic (yellow) planes are shown, too. b) Cross section of a typical CNC showing the number of chains it is composed of. Top and bottom surfaces mainly expose aliphatic bond, perpendicularly to the glucose ring plane. c) The shape of the CNC crystal might be either hexagonal (as in (b)) or octahedral as shown here and as suggested in ref. [29]. Adapted with permission.^[30] Copyright 2020, American Chemical Society.

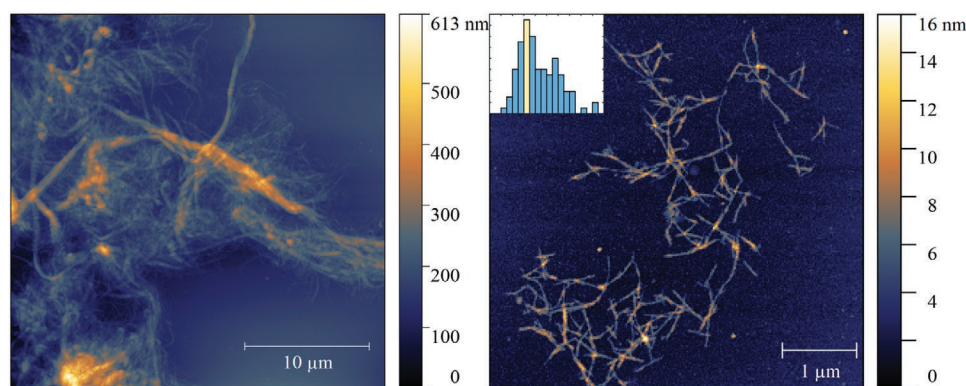


Figure 4. AFM images of (left) CNFs and (right) CNCs. The inset shows the histogram of CNCs length: each bin is 50 nm (total range: 0 – 1 μ m) wide and the most probable length (yellow bin) is 300 – 350 nm.

charged groups on the NC surface, and/or of coordinating multivalent cations in solution. Flexible microfibrillated cellulose and CNF entangle and assemble into weak gel networks just by mechanical treatments,^[45] while short sonication produces a network of weakly hydrogen-bonded rod-like CNC.^[46] All these gels, as the NC suspensions, are pseudoplastic materials characterized by a shear-thinning behavior.^[47,48]

The complex behaviour of the NC suspensions and gels and the dynamics occurring during the gelation processes have been recently re-investigated and discussed. Four phases (viscous liquid, viscoelastic liquid, repulsive glass, and attractive glass/gel) have been shown to exist over a composition range of 1 to 11.9 wt% CNC and 0 to 0.1 M NaCl.^[49] The understanding of NCs as colloids and the features of NC hydrogels and aerogels are out of the scope of this review. The physical and chemical cross-linking strategies to obtain NC hydrogels, to control gel structure, the hydrogel characteristics, and rheological properties have been extensively reviewed^[50,51] and the reader is suggested to refer to these publications.

Despite the rather favorable interaction with water, the hydrophilicity of NC is a questionable matter and an amphiphilic, rather than hydrophilic, nature is ascribed to NC.^[11,52] The concept is that lipophilicity is not necessarily the opposite of hydrophilicity, but must be similarly quantified by a chemical potential difference of an appropriately chosen “lipophile”.^[53] Accordingly, proof of the NC amphiphilicity was provided by the diffraction patterns of cellulose crystals and by computational studies which suggested that water molecules and hydroxyl groups are on the (110) and (010) faces of the cellulose crystal, whereas the relatively nonpolar C-H groups are exposed on the (100) face, facilitating the formation of solvation “gaps” on that surface.^[42] Upon drying, cellulose undergoes partly irreversible reorganization like aggregation or surface passivation to find the energetically most favorable state, a process named hornification.^[54] As a consequence, NC dewatering and drying processes pose several problems. The first is due to the cost of removing the tightly bound water. The second is related to the irreversibility of the process since the aggregation forces between CNCs and CNFs make it difficult to re-disperse the nanostructures upon re-hydration.^[11] Since performing a dewatering-drying process without loss of the nanoscale properties of NC is crucial for successful commercialization and also NC-based material

processing, various strategies have been developed. Current strategies are exhaustively described in a recent review.^[11]

NCs which have been directly dried from water, aggregate so that both the reactivity and nanoscale structure are lost with practical impact on applications of NC or ultrathin NC films. Johansson et al.^[27] suggested that the control of accessibility and reactivity of the NC hydroxyl groups is a route to resolve the challenges related to, for example, re-dispersibility of nanocellulosic materials and the NC behavior when subjected to air-drying as well as to different solvent media. Although dried CNF and CNC are hardly and incompletely re-dispersed in water, even after mechanical grinding and long-lasting sonication, hydroxyls allow the access of water inside the microfibrils^[55] and CNC films exposed to water vapors initiate asymmetric swelling since a “bilayer” of hydrated and dry NC is formed.^[56] This swelling produces an actuation movement of NC films. By measuring the absorption-desorption kinetics of D_2O by a CNC film, the water absorption was found very fast, since it ends in 2 min. Conversely, desorption is a slower process that is fitted by a bi-exponential law, supporting the presence of two independent water binding sites.^[57] The amphiphilic nature of NC and the localization of hydrophilic moieties (i.e., the edge of cellulose chains), which is different from that of the hydrophobic ones (i.e., the crystal face), allow NCs to behave as surface-active agents able to lower the interfacial tension at the liquid/liquid interface. Since NCs are colloidal nanosystems, when they irreversibly adsorb at liquid interfaces, produce a Pickering emulsion.^[58] These systems are discussed in more details in Section 5.2

3. From Nanocellulose Suspensions to Films

3.1. Overview of the Deposition Techniques

Hierarchical and high-order arrangements of molecules in assembled structures are common in biology. Wood, grass, and other cellulose-based materials are representative examples of structures where polymeric components form large, functional, and versatile constructs. CNCs and CNFs retain the ability to entangle and assemble of the native cellulose. However, being regular nanosized structures (in particular CNCs), with a large exposed surface where functional organic groups can be

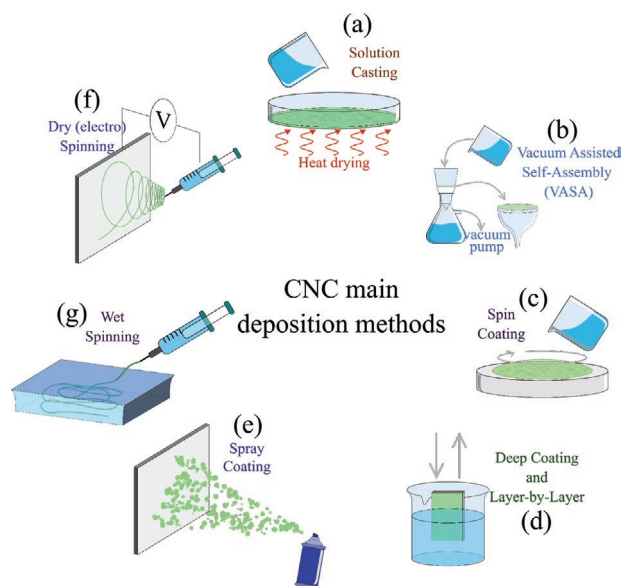


Figure 5. Cartoon view of the most common CNC deposition methods. a) Solution casting, b) vacuum assisted self-assembly, c) spin coating, d) deep coating and, more generally, layer-by-layer, e) spray coating, f) wet spinning, and g) dry spinning, eventually assisted by an electric field.

introduced, the self-assembly properties can be suitably modified. Moreover, due to Brownian motion in a colloidal suspension, the way by which NCs are left to arrange offers a further possibility to control the final structure. Several methods exist to deposit NCs with sufficient control over the final structure and arrangement of CNCs. The most common methods are sketched in **Figure 5** and their main characteristics are briefly described below. In general, when the solvent is left to evaporate from an NC suspension or an NC gel, a film is obtained. This process can be performed over a surface; in this case, the interfacial forces drive the NC self-assembly process and the surfaces work as templates. The basic experimental problems to be addressed for film fabrication are due to the film cracking during drying processes and the adhesion or, conversely the detachment of the film from the surface, if coating layers or free-standing films have to be obtained. Finally, the random versus ordered assembly of NCs inside the film strongly affects the physical film properties (see Section 5.2). Mild drying procedures and a choice of an appropriate substrate are the obvious aspects to be considered. However, the approach for film production remains the fundamental issue.

Early film preparations consisted of the conversion of a CNC suspension to a wet mat on a surface-hydrophilized polytetrafluoroethylene (PTFE) membrane with a pore size of 0.1 μm .^[59] Although there is a renewed interest in the vacuum assisted self assembly (VASA) approach (see Section 5.2), at present, the most common method to produce NC or NC composite films is solution casting.^[3] This method is simple, fast, cheap, and provides films of good quality. The drying step is usually carried out under moderate heating in a ventilated oven^[60]; however, drying in a desiccator cabinet under mild vacuum is more effective and allows to obtain more uniform thickness. Like all the drying process over a surface, the film features depend on the underlying substrate, in particular, on substrate roughness at

the micro-nano scale and on the affinity between NC and substrate itself. This last determines the feasibility of the peeling-off process and the selective distribution in the case of NC composites. For example, a selective distribution at the interface and the formation of a skin-like layer preventing diffusion was observed for a CNC chitosan composite gellified in a PET or Teflon mold.^[61]

In our experience, the most relevant parameter to obtain films with good quality is the NC suspension purity. In general, impurities induce NC agglomeration and in particular, salt impurities crystallize, which affects transparency, homogeneity, and gas permeability. In particular, in the case of CNC, a simple experimental trick is to perform an exhaustive washing step before filtration or casting. The limit of the filtration or solution casting approaches is that both CNC and CNF do not form large scale macroscopic ordered structures but randomly pack forming compact layers with, at most, localized nematic domains.

Control of film order and optical properties is achieved by more sophisticated deposition techniques. In spin coating, the solvent is removed by high-speed spinning of the solution on a substrate, and a solid film of NC is obtained with a high degree of reproducibility.^[62] Beyond the high degree of reproducibility, this method allows nanocrystal orientation and the films show birefringence properties tunable by varying the spin axis.^[63] Horizontal Langmuir–Schaefer deposition technique was used to attach NC to silica wafer previously treated with poly(ethyleneimine) (PEI) as anchoring polymer.^[64] Among the deposition strategies, the layer-by-layer (LBL) self-assembly of hybrid films by sequential dipping offers the best promise for the fabrication of functional thin films, providing accurate control over film thickness and film composition. NC is an excellent substrate since this approach exploits the molecular forces between the layers progressively deposited. In fact, NC fabrication procedures which require the chemical modification of some cellobiose hydroxyls introduce charged functional groups. Then, the appropriate choice of a spacer polyelectrolyte allows exploiting the strong electrostatic interaction between the opposite charges on NC and the spacer polyelectrolyte. The presence of attractive interactions of electrostatic (i.e., short range) nature between NC and the spacer layers is one of the main advantages of LBL since it limits the phase separation between the adjacent layers.^[65]

LBL-assembled films were prepared solely from CNFs, using alternate layers of negatively charged (i.e., phosphorylated) CNFs and positively charged (i.e., aminated) CNFs. These films showed excellent thermal stability and flame-protection characteristics.^[66] NC films obtained by LBL deposition find potential applications in a variety of fields and their current developments have been reviewed.^[8] In the authors' experience, a practical limit of this method is the contamination of the dipping solutions due to the release of the already deposited charged molecules or nanoparticles. If negatively charged CNC are deposited, a formation of a weak gel is observed following a further dipping in a solution containing positive electrolytes. In principle, this problem could be reduced by performing rinsing steps between each deposition. However, adsorption and diffusion of NC and polyelectrolytes at the film interphase is a rather complex process, and the rinsing results in worse film outcomes, such as reduced thickness and homogeneity.^[67]

The coating of a solid surface by spraying an NCs' suspension is an efficient alternative approach to obtain films of tunable thickness. The whole procedure is fast and necessitates standard laboratory equipment and can be performed on a bench scale. Reproducible films with a weight ranging from 52.8 ± 7.4 to $193.1 \pm 3.4 \text{ g m}^{-1}$ have been obtained by spraying an NC suspension on a moving smooth steel plate. The NC films showed a surface roughness of about 390 nm on the spray-coated side in contact with the steel plates and of more than 2 μm on the outside surface. This approach works efficiently also on permeable and porous substrates, such as paper or fabric. The spray coating of CNF on porous paper was shown to proceed by progressive steps: initially, CNF spots on the substrate, leaving residual large void pores, and thereafter, CNFs cluster around the fiber contact nodes in the paper substrate. Finally, the progressive thickening of a continuous film was observed.^[68] The permeability and mechanical properties of the substrates were shown to change according to these steps. Spray coating is a versatile approach by which, sheets, oil/water separation membranes^[69] or barrier layers have been obtained.^[68]

Another approach for the spray coating of aqueous slurries on wet substrates uses subsequent water removal by vacuum filtration. This process was applied to load porous paper with CNF, by using standard laboratory equipments and accurate control of the coating was obtained. It was observed that the CNF deposition proceeds according to subsequent steps: At first, the coating remains confined on the surface of the substrate forming irregular spots, then it clogs the pores, and finally, increasing the load, homogeneous films on the substrate are observed. The properties of the coated paper are strictly related to the film morphology and a drop in the air permeability together with a sharp increase in the tensile properties were observed only after the deposition of a continuous CNF layer. Conversely, the formation of cylindrical nanoscale structures was observed by airbrush spray coating of enzymatic cellulose on polished, hydrophilic silicon wafer surfaces. Methods from (a) to (e) (Figure 5) are sometimes grouped under the common name of evaporation induced self-assembly (EISA).^[70] Finally, the spinning methods use a nozzle to extrude a CNC by exploiting a specific driving force, generally either pressure or electric field. The wood-derived cellulose fibrils, which bundle into microfibrils with high aspect ratio, were used as stiff fillers of a biocompatible hydrogel matrix that swells readily in water.^[71] The hydrogel composite was then extruded through a deposition nozzle. A shear-induced alignment of the cellulose fibrils was observed and the printed filaments showed anisotropic stiffness, and, hence, swelling behavior in the longitudinal direction. Mesoscale architectures with programmable anisotropy and dynamic properties are created by the local control of the fibrils' orientation. The structuring of NC induced by 3D alignment,^[72] the different methods of 3D printing that could be applied to NC and its composites,^[73] and the challenging perspective in application^[74] in particular in the medical field^[75] have been recently reviewed. Among the most promising approaches for the deposition of oriented NCs is the direct ink writing, which is an extrusion-based, 3D printing combining high versatility with simplicity of operation. However, this method requires strict optimization of the

viscoelastic response of the ink, which depends on NC concentration together with the flow architecture. In this regard, a drawback is due to the limited concentration of NC that can be added to the inks. Monomer-based inks composed of 10 or 20 wt% CNC dispersed in solution containing various monomers were obtained improving the dispersibility of CNC as well as the interfacial bonding between particles, by modifying the CNC surface using methacrylic anhydride. In this way, the acetylation of the hydroxyls on the cellulose surface reduces the hydrogen bonding between the CNCs, allowing the solid loading to be increased from 10 to 20 wt%.^[76] The concentration of cellulose in the final printed material was increased by a wet densification process where the solvent molecules were displaced by direct attractive interactions between the –OH groups on the cellulose surface.^[77] Starting from the concept that the cohesive energy density of a material depends on the solvent it is dispersed in, the addition of these non-aqueous solvents into the liquid mixture will favor attractive interactions between the NCs. Since the efficacy of the added solvent in removing water molecules from the cellulose surface will depend on their polar character and hydrogen-bonding ability, ethanol and acetonitrile are effective in replacing the H₂O molecules from the cellulose surface and thus induce densification. By using inks with improved rheological performances, the fabrication of textured 3D structured composites with enhanced mechanical properties and other functionalities becomes feasible.

3.2. How Film Forming Conditions Affect Its Gas Barrier Properties

The natural propensity of NC to undergo self-assembly offers a possibility for the fabrication of highly performant bio-based films and coatings. However, the kinetic and thermodynamic of the assembly process, as well as motion of the NCs with both translational and rotational diffusion, determine the organization of the nanostructures and the film properties such as porosity, defects, fragility, and crack propagation. For this reason, the choice of the film fabrication method and parameters is of most importance. The most obvious property which depends on the fabrication method together with the NC morphology and surface charge is the selective gas barrier effect. A great deal of research is addressed at the enhancement of the barrier properties of NC-based films and coatings which are considered ecologically friendly substitutes of plastics packaging materials, in particular, to prevent food from spoiling during storage and delivering.^[78] Moreover, NC and its composites are expected to form molecular-sieving membranes which enable the precise separation of various gases based on their molecular sizes under moderate differential pressures, to be used in low-cost and energy saving systems.^[79] The permeability of a membrane to a gas is given by the product of the gas solubility and the gas diffusivity. The solubility depends essentially on the chemical nature of the membrane system; then the hydroxyl and oxygen containing groups along the NC surface should favor the permeation of polar gases. Indeed, CO₂ is much more permeable than O₂.^[80] and CNF membranes are promising systems for CO₂ capture, too.^[81] Conversely, the diffusivity depends mainly on the physical properties, such as

the material phase (i.e., crystalline regions) and porosity. In this regard, CNCs could be the best candidates for obtaining high gas barrier membranes.^[82] However, the possible gas pathways, their tortuosity, and the presence of void spaces play the major role. Flexible CNFs entangle into a web structure.^[83] In principle, CNCs could pack more tightly than CNFs, but the order and the packing depend on the rearrangement of these nanostructures during the film formation. In an earlier experiment, TEMPO-oxidized CNC membranes were prepared by suction filtration on a surface hydrophilized PTFE filter. The oxygen permeability of the filter was decreased to $2e - 3 \text{ mL } \mu\text{mm}^{-2} \text{ day}^{-1} \text{ kPa}^{-1}$ (by a $20 \text{ } \mu\text{m}$ thick layer).^[84] The permeability decreased further by increasing the crystallinity of CNC^[85] and was found lower than the experimental detection limit (that is $10^{-4} \text{ mL } \mu\text{mm}^{-2} \text{ day}^{-1} \text{ kPa}^{-1}$) when films were obtained by casting a low-ionic strength suspension of CNC at neutral pH on a polylactic film and drying at moderate temperature ($60 \text{ }^{\circ}\text{C}$ in an oven). AFM analysis indicated that the CNCs arrange with a loosed layer-by-layer structure with the CNC long axis lying on the plane of the film but with randomly azimuthal alignment, while positron annihilation lifetime analysis supported a high film compactness, with cavities in the range of 0.31 nm .^[80] It is reasonable to suppose that low ionic strength conditions favor the formation of hydrogen bonds between hydroxyls and carboxylates, while mild drying leaves time for CNC rearrangement, allowing to strengthen the hydrogen bond network and compacting the film structure. Void cavities having larger sizes were observed in the low-roughness hydrophilic ultrathin films CNF films obtained by airbrush spraying. These films showed switchable, tailored wettability, associated with the presence of two characteristic structural entities, with radius of 27 and 75 nm , which were attributed to the agglomeration of CNFs. By in situ humidification and drying of CNFs, these domains reversibly changed from 2D (cylindrical) to 3D (spherical) shape and the large pores or voids were either filled by water.^[86] By analyzing the relationships between gas permeability and anisotropy of nanocellulose films, it has been shown that high orientation of CNC films is critical to achieving the highest barrier performance and the O_2 permeability decreases by a factor of 900 between the isotropic and anisotropic films.^[87] Indeed, water penetration in the film cavities is the main issue for the exploitation of the gas barrier performances. In fact, although the competition of water is not strong enough to disaggregate the hydrogen bond networks, it is well assessed NC films lose their barrier properties once placed in humid conditions. Chemical and physical improvements of the fabrication procedures have been tried to tackle this issue. Inclusion of a second class of molecules, which provide electrostatic adhesion in general, improves the gas barrier performances. Film assemblies of PEI and NC, deposited on PLA as alternate layers by the LBL approach, were shown to increase oxygen and water vapor barrier properties significantly.^[88] Hydrophobization by coating the films with sol-gel,^[89] ester,^[90] and other water repellent molecules, or incorporation of polymers such as lignin^[91] could improve the film performances. Combining latex coating on both sides of the film with the increase of film density obtained by pressing at elevated temperatures, the films' swelling was strongly reduced even at $90\% \text{ RH}$.^[92] The here reviewed results prove the remarkable

achievements in the fabrication of NC films with gas barrier properties in the small laboratory scale; the feeling is that further development is still needed to extensively use these materials in the industrial field where easy, large scale and standardized fabrication procedures are necessary.

4. Reactivity of Cellulose and Interface Effects

Although the performances of the NC films in terms of the optical, mechanical, thermal, and gas-barrier properties are considered excellent, there is still significant room for improvement in the perspective of new emerging applications. The obvious approach consists in the introduction of chemical groups which adjust the interfacial properties of NC. Since the tuning of the NC properties is a fundamental issue for the effective production of NC-based materials, there is a huge amount of literature available on this subject. Several strategies to modify individual NC structures in solution exploiting organic chemistry or the interaction between NC and polymers or surfactants have been extensively reviewed.^[9,93–96] Herein, we focus on the problems arising from the peculiarity of NC and on the unconventional approaches aimed at engineering the NC's assembly or the NC's film interface properties.

4.1. Hydroxyl-Driven Cohesiveness and Reagent Accessibility

Cellulose consists of disaccharide repeating units where the breakdown process into nanoscale sometimes introduces functional groups such as carboxyls, phosphates, or sulfates. These groups are grafting sites for further modification. However, thanks to the large availability of hydroxyls, cellulose is readily functionalized through these reactive groups. The important issue to be faced is the limited accessibility of many reagents to the NC crystalline interphase^[27] which confines the reactive groups to the exposed surface. Moreover, the hydrogen bond network in the fibers' interior perturbs the partial hydroxyl charges and affects their reactivity. This problem concerns mainly the crystalline domains since higher hydroxyls' accessibility is expected within the amorphous regions.^[97] In this regard, the TEMPO-mediated oxidation was applied to various kinds of native celluloses, which have different characteristics in crystal structures and microfibril morphologies. The relationships between microfibril widths and amounts of functional groups formed by the oxidation (carboxylate and aldehyde groups) supported that, under the applied experimental conditions, the C6 primary hydroxyls exposed on the entire surfaces of cellulose crystallites or microfibrils were converted to carboxyls or aldehyde groups. Only in the case of cellulose I for the higher plant, the carboxylate and aldehyde groups exceeded the expected values, probably because the reaction partly occurred in amorphous or disordered regions.^[98]

In some cases, it is desirable to preserve the original morphology of NC and avoid the degradation of the native crystalline structure. In this case, the natural cohesiveness of cellulose chains helps to pursue the goal but makes it more challenging to ensure a sufficient degree of modification. More accessible and reactive functional groups should be produced by

oxidation processes that fringe the CNC structure and form short disassembled chains protruding from the ends. These trimmed hairy CNC have been proven suitable components of novel CNC networks^[99] and are expected to be more available for functionalization.

An alternative approach exploits the intrinsic reactivity of the reducing end groups of cellulose chains.^[100] Aldehydes undergo a variety of chemical reactions which can be used for the end-wise modification of the chains, or for grafting NC to polymers or surfaces by one end. Different end-wise reaction routes have been proved to be effective on NC, despite that in the dry state (i.e., in the NC films) and in part also in aqueous solutions, the reducing ends are present as hemiacetals.^[101] These modification routes have been reviewed in detail.^[102] The main advantage of the end-wise modification of NC is that it makes even more important the natural directionality of the cellulose chain; meanwhile, it does not alter the NC surface chemistry and properties. For these reasons, this approach offers interesting opportunities for one-site grafting of CNC or the fabrication of ordered and aligned monolayers.^[103] Conversely, the selective and localized wise-end modification is not suitable for changing the massive properties of NC and NC films.

4.2. Agglomeration and Reaction Media

The affinity of NC for aqueous environments and its tendency to agglomerate in non-polar media represent a rather intriguing problem to apply classical organic chemistry reaction routes which usually require anhydrous solvents. Several approaches have been proposed to disperse NC in suitable reaction media. From a theoretical perspective, Ferguson et al. observed that NC behaves like other insoluble 1D materials, such as single-walled carbon nanotubes and nanowires, which in organic dispersant media aggregate by van der Waals driven interactions. Then, a thermodynamic framework could be used to predict the best dispersants for NC, that is, the best solvents should possess surface energies that match the surface energy of the nanomaterial itself.^[104] From an operational perspective, the NC transfer from water to organic dispersant media was made possible by using NC obtained from selected sources such as tunicates,^[105] coating NC by surfactants,^[106] freeze-drying the aqueous suspension and then dispersing the material in the organic media with the aid of sonication,^[107] solvent exchange in liquids of decreasing polarity,^[108] or substituting the counterion of carboxylate groups of TEMPO-oxidized CNC.^[109] Increasing attention has recently been paid to the use of ionic liquids to disperse cellulose and its derivatives.^[110] Ionic liquids and deep eutectic solvents are composed of organic cations and organic/inorganic anions and can be performed up to full dissolution of cellulose by a hydroxyl driven process.^[111] Imidazolium-based ionic liquids have been proven to be efficient solvents to extract NC from raw materials^[112] as well as to perform reactions involving hydroxyls.^[113] In particular, by using ionic liquids under dilute conditions with concurrent acid hydrolysis, CNCs were obtained directly from cotton gin notes.^[112] A process performed in ionic liquids that could simultaneously induce lignocellulose delignification, in situ hydrolysis of amorphous cellulose, while keeping cellulose native crystalline parts undamaged have been described.^[114]

Deep eutectic solvents containing ammonium formate as the main hydrogen bond acceptor and an organic acid (glycolic, lactic, or levulinic acid) were successfully used as a cellulose-dispersing agent; meanwhile, positive groups were introduced in the cellulose chains by reductive amination. By this method, amorphous cellulose domains were partially dissolved by undergoing aminolysis, resulting in the formation of water-dispersible, positively charged CNC with high crystallinity.^[115]

4.3. Available Reactive Groups and Functionalization Routes

Acylation,^[116] acetylation,^[117] esterification,^[118] silylation,^[119] amidation,^[120] and other well assessed organic chemistry reactions have been adapted to NC modification. Due to the extensive literature reported on this subject, several protocols have been set up and commented in the published reviews.^[9,94,121] Hereinafter, we cite or comment just some research papers reporting protocols which are effective in our personal experience or are at the frontiers of nanocellulose modification.

Recently, an increasing interest is addressed toward thiol-ene chemistry,^[122] and triazinyl group chemistry using cyanuric chloride as linker molecule to produce cellulose ether derivatives.^[123] These are versatile modular approaches for:

- 1) tuning the interfacial properties of NC;
- 2) enabling its dispersion in a range of solvents;
- 3) forming homogeneous colloidal suspensions that are stabilized through electrostatic and steric interactions;
- 4) providing grafting points for covalent attachment of NC to other polymers, nanostructures, or surfaces.

The thiol-ene chemistry was proved to be effective to tailor the wettability and moisture sensitivity of CNF films by the two-step procedure shown in **Figure 6**. In the first step, the films were coated with a layer of reactive nanoporous silicone nanofilament by polycondensation of trichlorovinylsilane that introduces both nanoscale roughness and reactive vinyl groups. In the second step, the films were functionalized via photoclick thiol-ene reaction. Photomasking allowed preparing superhydrophobic/superhydrophilic patterned surfaces, while transparent slippery omniphobic CNF films were obtained with perfluoropoly(propylene oxide) lubricant (Krytox 103) which displayed repellency against both aqueous and organic liquid with surface tensions as low as 18 mN m^{-1} .^[124] Thiol-ene chemistry together with photomask-assisted micro-patterning was successfully used to tailor the surface of cellulosic substrates and NC films. To this purpose, alkyne moieties were introduced in the substrate for the subsequent photo-induced coupling of thiol-containing molecules. Photomask-assisted micro-patterning of the functionalized substrate was obtained by UV lithography, to realize spatially-resolved designs of surfaces with different properties.^[125]

The thiol-ene functionalization was successfully utilized to produce core-shell nanostructures with phase-change properties. This nanomaterial consists of a CNC core and a soft shell of octadecyl chains. The alkyl chain was introduced in two steps: First, 10-undecenoyl chloride was left to react with CNCs hydroxyls in pyridine. Then, 1-octadecanethiol

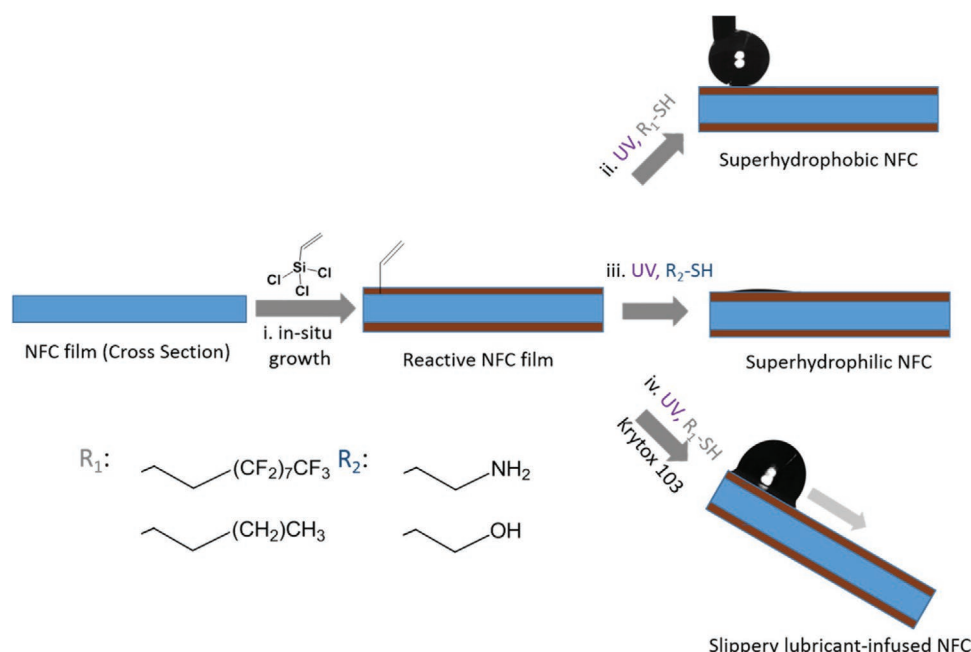


Figure 6. Functionalization of films of CNFs. Trichlorovinylsilane grafts and polymerize on the film surface where it forms nanofilaments carrying reactive vinyl groups are grafted on the surface. i) The vinyl groups can be reacted with thiolated compounds carrying hydrophilic or hydrophobic groups via photoinduced thiol-ene click reaction (ii and iii). The fabrication of slippery, liquid-infused porous CNF film surfaces can be achieved by impregnation of porous CNF films that have been fluorinated by the thiol-ene click reaction with a low-surface-energy, chemically inert lubricant (iv). Adapted with permission.^[124] Copyright 2016, American Chemical Society.

was grafted in the shell layer containing terminal vinyl groups via thiol-ene reaction. The solvent casting of the suspensions of these modified CNCs (C_{18} -UCNCs) on Teflon support produced self-standing films (Figure 7a,b) that, after being peeled-off, become nontransparent and superhydrophobic (Figure 7a, inset) since synergistic phase segregation

is driven by the shell (octadecyl) chains which lead to the crystalline structure within the flaky units as confirmed with small-angle X-ray scattering curves (Figure 7c). The phase transition of the shell conferred on the flaky structures superior thermoinduced self-healing and thermoreversible properties (Figure 7d).^[126]

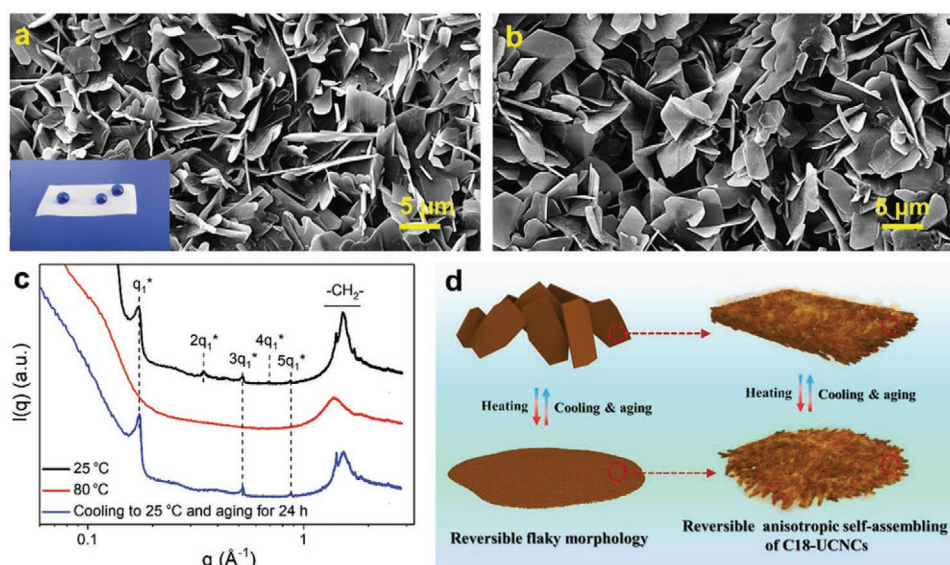


Figure 7. Flaky self-assembled structures by C_{18} -UCNCs. a,b) SEM images of flaky self-assembled structures on the top surface (a) and the bottom surface (the surface in contact with Teflon during film formation) (b) of the as-prepared C_{18} -UCNCs film. The inset in (a) shows the dyed water droplets on the surface of the C_{18} -UCNCs film. c) SAXS curves of a C_{18} -UCNCs film measured under different conditions: as-prepared films at 25 °C, heated at 80 °C and cooled from 80 to 25 °C and aging for 24 h. d) Schematic of the formation of a thermoreversible flaky structure. Reproduced with permission.^[126] Copyright 2020, Wiley-VCH.

4.4. Gas Phase Route and Plasma Functionalization

Gas-phase treatments are an attractive alternative to avoid the transfer in organic solvents and reduce the amount of the reagents and toxic wastes. Moreover, gas-phase reactions aimed at surface modification can be performed directly on solids such as films. A gas-phase reaction was successfully applied to hydrophobization of micro fibrillated cellulose by hexamethyldisilazane, by using simple and cheap laboratory equipments.^[127] Depending on the characteristics of the reactants, the passage from liquid to vapor phase could require low pressure and the experimental set-up must be equipped with a vacuum chamber and pumps. An alternative approach is based on plasma treatments that have been applied to cellulose and its derivatives in the form of films or sheets. Gaseous plasma is a well-established system for the modification of polymeric materials and surfaces. However, plasma treatments produce chemical but also physical changes to the surface properties and could affect the buried interfacial structure. The wettability of a thick cellulose film was increased by a dielectric barrier discharge plasma operating in both, air, and an ammonia/nitrogen gas mixture. However, in spite of the changes in the surface functional groups, that is, amine and amide moieties were grafted, the wettability was related to the structural changes (i.e. the increased surface roughness^[128]). Microwave Ar plasma treatment of cotton fabric induced an opposite change of hydrophilicity depending on the experimental conditions. This opposite change was associated with a change of crystallinity and of the cell unit parameters of cellulose, such as intrachain glycoside bonds and intra and inter chain hydroxyl hydrogen bonds.^[129] Nanocomposite films made of BNC and poly(3-hydroxybutyrate) with a thickness of 200 μm were plasma-treated for increasing their hydrophilicity and then coated with ZnO nanoparticles dispersed in an alcohol solution using an ultrasonic spraying device. Under the conditions of this work, the thermal stability, crystallinity, and melting behavior of nanocomposites were not changed by the plasma treatment; however, a remarkable increase in stiffness and strength was obtained. Moreover, the ZnO coating provided a strong inhibition of bacterial growth.^[130]

An innovative approach exploits the potentiality of submerged liquid plasma (SLP). SLP, which is performed in the liquid phase, is environmentally friendly and requires low temperatures and simple and low-cost equipment. This technique initiates specific reactions at the liquid/plasma/nanoparticles interface and then may contribute to break the bonds on the NC surface. By a plasma treatment with a torch completely immersed in dispersions of microcrystalline cellulose (MCC) in water or acetonitrile-water mixtures followed by ultrasonication, it was possible to obtain the simultaneous defibrillation and functionalization of the MCC. In particular, amines, ketones, and aldehydes were introduced on the surface, while the MCC backbone was not significantly disturbed.^[131] This approach was effective also on nanocellulose fibers dispersed in water.^[132] The gas-phase reactions allow obtaining Janus-like films with interfacial activity, being the two film's sides chemically different from one another. Selective one-side introduction of carboxylic functionalities on CNC film was obtained by a simple two-step procedure. The first step consisted in the pre-modification by periodate oxidation of CNC. This is a well-assessed reaction

that introduces aldehyde functionalities. These modified CNCs interact also through intra- and intermolecular hemiacetal and form films with superior mechanical performances. The one-side conversion of the aldehyde groups to carboxyls was done by exposing the film to ozone on one side while blocking the gas passage from the film sides with glass slides. The gas-phase ozone treatment was proved to be efficient but not disruptive since the film properties were completely preserved.^[133]

4.5. Enzyme Mediated Functionalization

An alternative route for NC functionalization exploits the performances of biocatalytic systems, that is, enzymes and microorganisms. The biocatalytic approach has a great potential to address the major challenges of NC production and functionalization: These processes are performed in aqueous media, require a low energy expenditure, and the release of toxic wastes is limited. Several enzymes catalyzing transformations of carbohydrate (or other biopolymers) could be found in nature, and great advances have been made by the bioengineering approaches to obtain large amounts of these biomolecules or whole cells and microorganisms with optimized stability and catalytic performances. The most promising NC transformations catalyzed by enzymes have been reviewed.^[134,135] The oxidation of C₆ hydroxyl of the glucose units to aldehyde or carboxyl by molecular oxygen, catalyzed by the enzyme Lacase, according to the method proposed by Aracri et al.^[136] was successfully applied to produce films of bacterial NC with improved mechanical properties while maintaining barrier function.^[137] The reaction yield in terms of grafted carboxyls (140 $\mu\text{mol g}^{-1}$ of cellulose) enabled the interaction of the CNF with Ag ions and the generation of silver nanoparticles. The reaction was performed at neutral pH and is an advantageous alternative to the TEMPO catalyzed oxidation combined with NaBr/NaOCl^[33] which requires an aggressive agent (NaClO) and is performed under alkaline conditions. In our opinion, the enzyme or microorganisms catalyzed process could be one of the transformation routes of NC of the future. However, much has still to be done to decide which reaction is suitable for the desired functionalization, to screen the enzyme variants and set up versatile protocols providing an acceptable extent of NC's modification. Finally, since the aim is to scale up the processes to industrial applications, the enzyme performances and the enzyme availability in large quantities should be optimized by molecular bioengineering approaches.

4.6. Tuning the Film Properties without Post-Processing: The Hemicellulose Coating

All the methods aimed at obtaining NC films with better performances use purified NC which was obtained with a more or less harsh process consisting of chemical treatments to pass from coarse material sources (such as wood) to cellulose followed by the mechanical and/or chemical top-down processing. Then, NC is chemically modified. A different strategy has been recently proposed to obtain CNF nano paper with superior mechanical properties and high optical transmittance.^[138] The

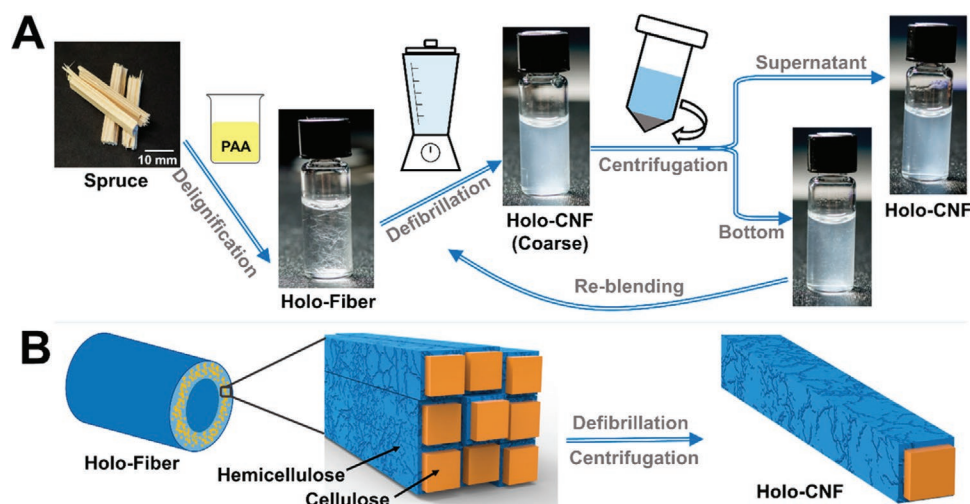


Figure 8. a) Overall processing route from spruce wood to Holo-CNF, comprising PAA delignification, defibrillation (using blender), and centrifugation steps. The bottom fraction after centrifugation was rescued for more rounds of defibrillation to increase the yield of Holo-CNFs. b) Schematic representation of core-shell structure Holo-CNFs obtained from Holo-Fiber. Reproduced with permission.^[138] Copyright 2019, American Chemical Society. (<https://pubs.acs.org/doi/10.1021/acsnano.9b07659>, further permissions related to the material excepted should be directed to the ACS).

idea underlying this innovative approach is to use a less aggressive treatment to pass from wood to CNF so that the natural coating of the fibers is retained. Indeed, as shown in Figure 1, wood cellulose is naturally coated by hemicellulose. Hemicellulose is highly hydrated and bears a negative charge due to glucuronic functionalities so that in aqueous solution the hemicellulose layer maintains the fibril separation via steric hindrance and charge repulsion and the hemicellulose-coated CNFs (holoCNFs) form a stable colloidal suspension. In synthesis, using spruce as starting material, a mild delignification was performed by peracetic acid and the holoCNFs were readily defibrillated by a low-energy kitchen blender as shown in Figure 8. The holoCNFs could be a versatile and low-cost form of NC suitable for several applications.

5. Interface Engineered Applications of CNC-Based Materials

5.1. Crystallization Induced by CNC

The control over thermodynamics and kinetics of crystallization is of paramount importance for a broad range of applications. In fact, the possibility to control the polymorph of the crystallizing compound is fundamental to increase the performances of catalytic sites, the bioavailability of active pharmaceuticals ingredients (API), and to create nanostructures with desired optoelectronic properties, to cite but a few.

Most often crystallization starts from a heterogenous nucleation event induced by a foreign phase (either a solid impurity present in the solution or a container surface).^[139] This fact implies that heterogeneous nucleation is the most powerful strategy to pursue to control the product of the liquid to solid phase transition. So far, rigid and nanostructured materials have been the platform to study heterogeneous crystallization (nanopores, patterned inorganic substrates, etc.), yet soft materials show many promising properties that render them more

flexible in these types of studies. In fact, compared to rigid nanostructures, crosslinked polymers and hydrogels have several tunable parameters: from their mesh size and rigidity^[46] to the polymer-solvent interaction. For example, it has been demonstrated that, by controlling the solute-polymer interactions, the partition function of the compound to crystallize can be modified to concentrate it into specific regions of the gel structure.^[140]

The first studies of crystallization in gel date back to the 60s^[141] but the interest in this research is constantly increasing since the steadily improved control on nanostructures permits a finer tuning of the crystallization strategies.

In this line, cellulose hydrogels have a further aspect of interest: since the CNCs are rigid elements, their highly crystalline structure provides a reproducible substrate to study the crystallization events and they ease the understanding of their interactions as these can be precisely modeled at different length scales: from all-atoms^[142] to coarse grain approaches.^[143]

The use of CNC for such studies has been investigated both in fundamental and applied studies to characterize the dynamic of crystallization of polymers induced by CNC. For example in refs. [144, 145], the authors studied polylactic acid crystallization induced by CNC using PEG as plasticizer. The authors find that both CNC and CNF ease the polymer crystallization and produce higher crystallinity compare to commercial nucleant. Other studies aim to develop composite materials with improved mechanical characteristics.^[146] In this case, surface acetylation of CNC produces a partial amorphization of the CNC surface that increases its miscibility with the polyester and acts as antinucleation agent. On the other hand, pristine CNC increases the crystallization temperature since its surface promotes heterogeneous nucleation. In another study, similar results in term of increased nucleation site density are reported for CNC in polycaprolactone; yet in this case, the large concentration of CNC in the polymer matrix (up to 10% w) limits the polymer crystallinity. Typically, since the dispersed CNCs act also as filler, an increase in their concentration produces

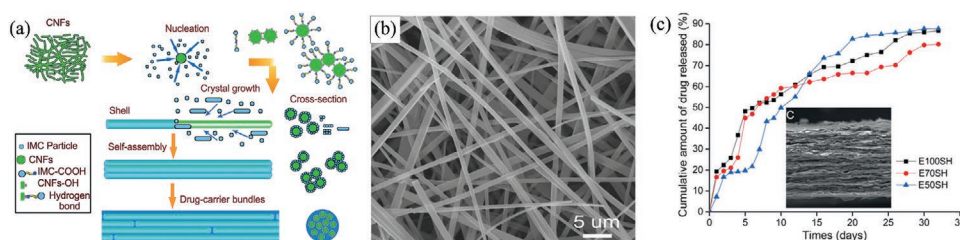


Figure 9. a) Mechanism of formation of the composite CNFs/indomethacin material: the nuclei of indomethacin nucleate forming a shell around the CNFs. These elements self-assembly into micron-sized large fibers. b) SEM picture of the composite fibers. c) Kinetic of release of the drug from three samples differing in the composition of the solvent used to prepare them. Adapted with permission.^[149] Copyright 2014, Wiley-VCH.

large storage moduli but reduces the material toughness. For example in ref. [147], the authors propose an in situ polymerization strategy to create nanocomposite of poly(ethylene succinate), and they found that the addition of up to 0.25% w of CNC increases both the crystallization rate and temperature of the composite while maintaining the tensile properties.

To note that also the polymorph structure plays a role in defining the final properties of composites materials, most probably because of the different interfaces they create. In ref. [148], a composite of CNC and chitosan is formed and the authors studied how the polymorphs cellulose I and cellulose II affect the mechanical properties. They found the cellulose I produces the best results notwithstanding the larger size of the CNC particles.

Fine control over crystallization is of large importance in pharmaceuticals where a major concern in developing new APIs is their solubility. To address this limit, a possibility is to exploit crystallization-induced effects to obtain either higher energy polymorphs or amorphous forms having greater water solubility.^[150,151] In refs. [152, 153], the authors graft primary amine of variable chain length to CNFs to create a hydrophobic solvation region around CNC to ease the crystallization of poorly soluble APIs. The results were promising as some of the compounds investigated effectively nucleate to solid form (either as crystalline or amorphous). In ref. [149], the authors demonstrate the self-assembly of CNC and a hydrophobic molecule (indomethacin) into microscopic ribbon with good encapsulation and drug-delivery properties. **Figure 9a** sketches the mechanism of formation of the ribbon, in (b), typical ribbons are imaged with SEM and panel (c) reports the kinetics of the release of the drug.

Another example of the strong interactions happening within the hydrogel matrix is demonstrated by the experimental releases of non-polar beta-carotene (BC) from NC hydrogels.^[154] The BC has been co-loaded together with a surfactants (Tween80) inside NC hydrogels. The release curves in water show a nearly quantitative release of the loaded BC only if the drug is co-loaded with the surfactant (red curves of **Figure 10a**). No BC was detected without surfactant. The drug released shows the typical BC absorption spectra (red curve of **Figure 10b**) but with a strong absorption tail in the UV. Since this tail cannot be ascribed to the surfactant, not even at concentrations well above its critical micelle concentration, the author hypothesizes that BC contained inside Tween80 micelles is released and that the UV tail was due to scattering from the micelle cores. In fact, by extracting the BC in an organic phase (hexane) and by disrupting the micelles with a strong sonication treatment, the UV tail of the BC absorption spectra disappears, supporting the idea that the hydrogel favors the formation of BC micelles during the release. The study reports also improved storage of the BC in NC hydrogels compared to the same molecule kept in freezer (after 45 days the amount of BC quantified spectrophotometrically was 92% vs 78%, respectively). Finally, albeit not directly related to crystallization events, CNC and CNF have been studied also as interfacial stabilizers between immiscible polymers. In ref. [155], both CNC and CNF were used to improve the interfacial miscibility between poly(vinyl alcohol) and poly(ethylene oxide) blends. The composites material added with NC shows increased mechanical properties and no degradation of thermal stability.

Despite a large amount of work on this topic, there is still a lack of general rules to better exploit the possibilities given

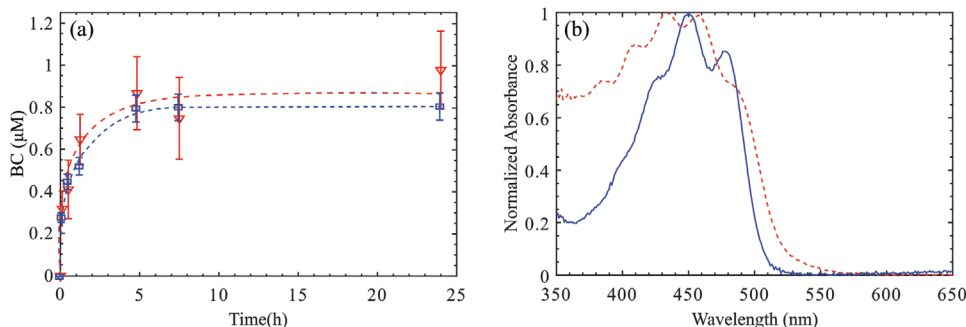


Figure 10. a) Release curve of BC in water (blue squares) and after extraction in organic phase and micelle (red triangles). Curves are guide for the eyes. b) Absorption spectra of the BC in water (blue curve) and in the organic phase (red continuous curve). Adapted with permission.^[154] Copyright 2019, University of Trento.

by CNC stimulated heterogeneous nucleation. For example, the following are some of the topics that need a more in depth investigation: The behavior of cationic CNC as nucleation substrate is poorly investigated as it is only discussed in ref. [156]—the Lindman hypothesis should be carefully verified to understand if and to which extent the amphiphilic nature of CNC affects the crystallization processes.^[52] There is still no consensus on how the different crystalline forms of cellulose affect the dynamics of the crystallization and if specific crystalline planes favour/inhibit nucleation/crystallization events.

5.2. CNC-Based Pickering Emulsions

As for any colloids, the stability of CNCs suspensions depends on the resultant interactions among all the forces involved between the colloidal particles and the solvent they are immersed in. The celebrated DLVO theory^[157] explains the main phenomena occurring: The long-range dipolar and steric interactions highly depend on the size and shape of the colloids, pH and solution ionic strength. The repulsion force between colloids with similar charge (as CNCs) scales as the Debye–Hückel screening distance while the (mostly) attractive van der Waals interactions scale with a larger exponent power law and only slightly depend on the physico-chemical details of the system (roughly speaking, since they account for the reduced surface area upon contacting two interfaces). Thus, colloids form stable emulsions if the repulsive forces dominate over the short-range ones and tend to flocculate in the opposite case (albeit with complex dynamics). A recent review on the topic is in ref. [158].

Pickering emulsions refer to emulsions stabilized by nanoparticles that make no use of surfactants. Pickering emulsions might be more stable and less toxic than surfactant-based.^[159] Double Pickering emulsions have been prepared too.^[160]

As a first approximation, the decrease in free energy due to particle absorption follows from the equilibrium of the interacting surface forces,^[161,162] but a more complete description of the behavior of the interface should consider also the deformation energy and some models have been recently proposed to tackle this issue.^[163–165]

Yet, if the curvature radius is not “too small”, the Young–Dupré equation still describes the main effects, and it demonstrates that moderately wettable particles produce the most important decrease of the system free energy while, for example, superhydrophilic particles produces no energy decrease. When the contact angle is $\approx 90^\circ$, the particle is easily trapped at the interface and the work required to remove it from there might be orders of magnitude greater than the thermal energy.^[166] This is the main reason that solid nanoparticles act effectively as an emulsifier in forming Pickering emulsions and can create emulsions much more stable than those based on molecular surfactants that are not subjected to the desorption energy barrier and more prone to coalescence.

At a liquid–liquid interface between two immiscible phases (e.g., polar–nonpolar), a hydrophilic particle will sink more into the hydrophilic phase to minimize its surface excess energy, thus reducing its contact angle into this phase. The opposite will work for hydrophobic particles.^[58,166,167] The effect is schematized in **Figure 11** where δ indicates the contact angle of an ideal planar surface having the same orientation of the CNC

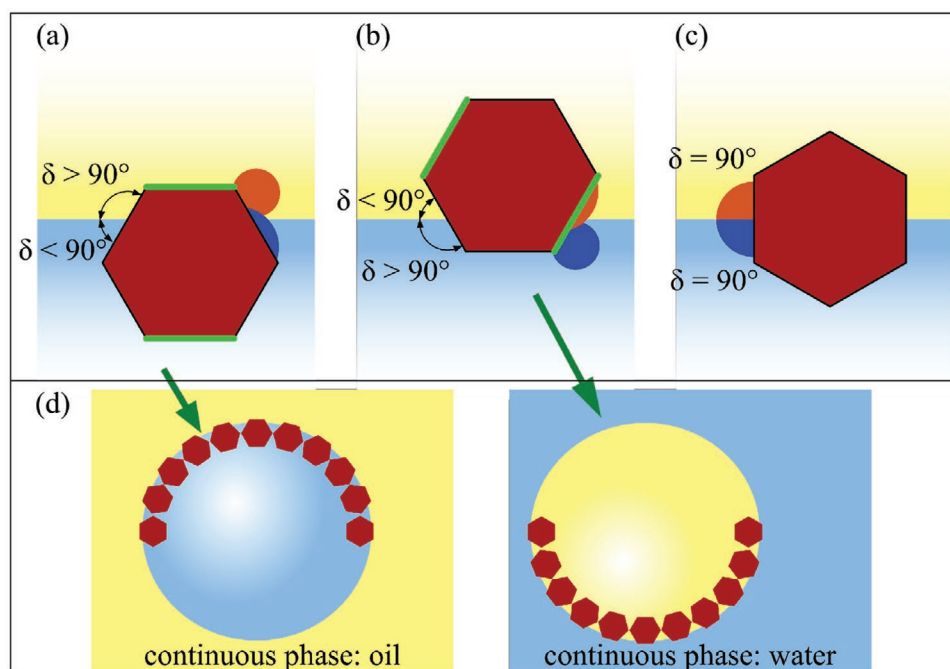


Figure 11. Scheme of the orientation of a colloid at the interface between immiscible liquids. a) An hydrophilic colloid will sink into polar medium (cyan) so to maximize its coverage with a polar media and to reduce the interface energy. b) For the same reasons, a lipophilic particle will be mainly wetted by the non polar medium (yellow). c) The ideal case of a truly amphiphilic particle sitting halfway between the media. Orange and blue drops schematically represent how a nonpolar (orange) and a polar (blue) medium would wet the solid surface; non polar surfaces are in green. d) Pickering colloids stabilize the formation of the droplets of the medium they are more affine to (Bancroft's rule).

(schematized here as of hexagonal cross-section). The orange and blue shapes indicate the shape of a lipophilic and of a hydrophilic drop, respectively. This effect is known as Bancroft rule^[168] and it implies that hydrophilic particles will tend to form O/W systems, while hydrophobic ones will preferentially form W/O.

Unconventional emulsification can be obtained by mixing the hydrophilic nanoparticles into the oil phase.^[169] In fact, since it is known that O/W interfaces are negatively charged, the energy barrier to cross the OW interface is greatly reduced without the need to change pH or ion strength (both strategies might not be compatible with real case industrial processes).^[170–172] Yet, this strategy has not been used with CNC/CNF.

CNCs/CNFs have been used to stabilize all types of emulsions (O/W, W/O, and W/W), with the first case using native (hydrophilic) CNC; the second exploits surface functionalization strategies to CNC increase hydrophobicity^[173]; and the latter, albeit it does not exploit the Pickering effect, uses the immiscibility of the two polymers aqueous solutions in which CNCs are dispersed.^[174]

Experimental results report the existence of a significant lag time for CNCs adsorption at the liquid–liquid interface,^[175] meaning that a remarkable kinetic barrier has to be overcome. Such barrier can be reduced by either increasing the concentration of CNC (typically up to about a few % wt) or by the electrostatic screening of the CNC surface charges by increasing the solution ionic strength.

The amphiphilic structure of NC eases the emulsification properties by allowing the CNC to reorient into the most energetical favorable condition at the liquid–liquid interface and broaden the possibility to effectively emulsify the system.^[30,41]

CNCs have been used also to inhibit emulsions for example to remove water from oil^[176,177]; in this case, the greater affinity of CNC with the water phase is used to destabilize unwanted emulsion and recover a purified product with limited use of chemical and energy-intensive treatments.

The stability of Pickering emulsions depends on several systems parameters and no exact rules exist to predict the behavior of a solid emulsifier in a given system. Some aspects are of general validity and apply to most of the systems, irrespectively, of the chemo-physical details.^[168]

The use of CNC for stabilizing water-in-oil emulsions is less studied mainly because the low CNC solubility in organic solvents generally requires a proper surface functionalization to render it compatible with the non-polar phase. Yet the availability of biodegradable, non-toxic, and biocompatible emulsifier for O/W systems is an important field as they find application in food and cosmetics industry. CNC Pickering for O/W are reported for hydrophobic-CNCs.

The fact that CNC has found no application as Pickering stabilizer in W/O emulsions is probably due to the relative orientation of the CNCs at the W/O interface and on the way they pack together to stabilize it. A recent work investigates this topic and nicely quantify several interfacial and interaction energies for CNCs reorientation at both solid and liquid interfaces.^[30] Yet, the work only speculates details of interfacial alignment of CNCs and several convincingly conformations exist and support the broad values of experimental results.

It is known that the size of the droplets decreases by increasing the CNC concentration since the energy released by

the emulsifying process typically creates much large interface area than that can be stabilized by the amount of emulsifier present. Thus, small droplets coalesce forming larger ones until a sufficient coverage of the interface by CNC is achieved.^[178] The charge density of CNCs seems to be the most relevant parameter to stabilize the interface, irrespectively, of the source and of the CNC polymorph considered. A limiting value of 0.03 e nm^{-2} has been reported, but this value depends on the solution ionic strength since the screening effect permits the formation of emulsions also for higher charged CNCs.^[179]

Oil-in-water but also water-in-oil and oil-in-water-in-oil double emulsions were successfully stabilized by CNF and cellulose CNC eventually esterified with lauroyl chloride according to a topochemical modification.^[160] In this case, four different double emulsions were prepared by combining two non-modified nanomaterials (CNC and CNF) to be used for the inner interface (oil/water) and two modified nanomaterials CNC-lauryl modified and CNF lauryl modified for the outer interface (water/oil). Because of their easily scalable production processes, the loading capability with essential oils, as well as cost-effectiveness, these emulsions are finding increasing applications for incorporating essential oils in food.^[180]

5.3. Piezo- and Tribo-Electric Effects

Cellulose is known to possess a significant piezoelectric response arising from its highly polar and non-centrosymmetric structure. The availability of NC films and composites materials permits the realization of electromechanical harvesting components (EHC). These are devices exploiting different mechanisms (piezo-, tribo-, pyro-electric, etc.) to generate and accumulate the charge produced by stochastic (eg. non-periodic) stimuli. Furthermore, since these stimuli generate broad types of current pulses, a controlled coupling among the electromechanical effects will improve EHC properties (e.g., see tribo vs piezo^[181] vs electromagnetic generators^[182]).

It is estimated that human daily activities (e.g., walking, breathing, etc.) reach power levels of about 100 W .^[183] Despite several high-performing EHC have already been developed and integrated into Internet-of-Things systems, the field of environmentally friendly EHC, based on sustainable materials and technologies, is still in its infancy. EHC can reduce the energy footprint of devices consuming small amount of power by recovering significant amounts of power from vibrations, rotations, mechanical deformations, and frictions happening every day in environments we are interacting with (e.g., wind, water flow, etc.). The possibility to harvest tiny amount of energy from these frequent events is an emerging trend that can support more effective green energy technologies and EHCs might lead to the fabrication of self-powered devices exploiting, for example, the human body to work.

The first studies about piezoelectric effect in cellulose dates back to 50s^[184] and several applications of cellulose in this field have been reported.^[185–189]

Piezoelectric effect refers to the development of a voltage drop across a material upon applying a pressure that produces a deformation of the material lattice and its consequent polarization.^[190] **Figure 12a** displays a schematic view of a

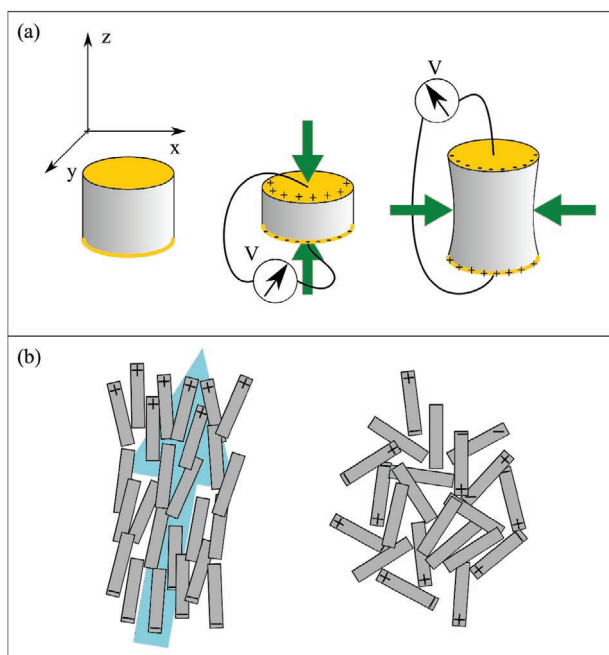


Figure 12. a) Schematic view of piezoelectric induced voltage drops. b) Alignment of (supra)molecular dipoles is essential to induce a macroscopic material response.

piezoelectric material that, upon compression, develops an electrical potential difference across its surfaces. Figure 12b exemplifies the need for an alignment of electrical dipoles to develop a macroscopic polarization state on the material surfaces. The induced polarization creates charge densities on the surfaces of the piezo-material that, upon electrical connection, are balanced by the electron flow across the external load. The current induced by the polarization field is the polarization term of the Maxwell displacement current; thus, the simplified scalar version of the constitutive equation for the piezoelectric current reads:

$$J_{D_z} = \frac{d\overline{P_z}}{dt} = \frac{d\sigma_p(\Delta h)}{dt} \quad (1)$$

where J_{D_z} is the displacement current due to the time derivative of the polarization field induced along the z axis ($\overline{P_z}$) due to the stress $\sigma_p(\Delta h)$ applied along the same axis. To note that J_{D_z} is proportional to the material deformation (Δh) along z as well as to the rate at which the material is deformed. In this equation, we simplified the tensorial nature of the constitutive equations and assumed that no electric fields are present and that the material response is isotropic in the (xy) plane. From Equation (1), via Ohm's law, the displacement current can be derived in terms of geometrical system parameters (i.e., electrode area, material permittivity, external loads, etc.).

Although the piezoelectric effect is the most studied one, others effects can be successfully exploited to produce energy. For example, triboelectric generators develop a surface polarization state of adjacent material interfaces due to the different electrochemical potentials of the dielectric materials. A periodic relative motion between interfaces (either contact/separation or

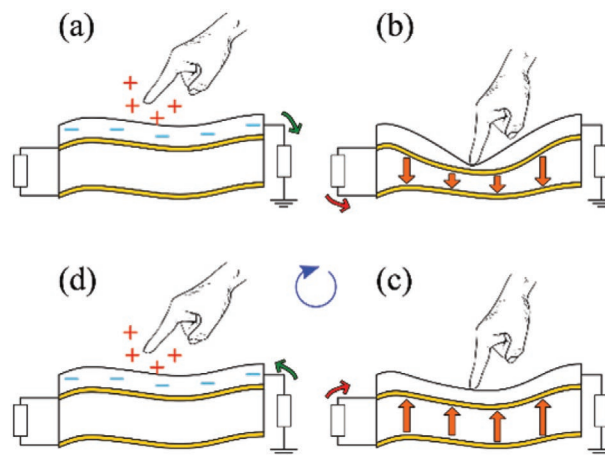


Figure 13. Sketch of the operating principle of a piezo-tribo EHC. The top layer exploits the triboelectric generation, while the bottom layer is a piezoelectric material: a) during the contact phase, the triboelectric effect comes into play; while during both deformation and relaxation phases (b,c), the piezoelectric operates. Finally, during the “detachment” (d), the reverse tribo-effect is generated.

transverse friction) induces displacement current that is measured as pulses flowing across external loads.

Coupled piezo and tribo-generators have been recently demonstrated^[191–194] and their behavior is sketched in **Figure 13**.

So far, only two papers tackle the possible origin of CNC piezo-effect: DFT simulations are carried on in ref. [195] following the more general result arising from the intrinsic piezoelectric of hydrogen bonds,^[196] which support the idea that the piezoelectric originates from the in-plane alignment of the anhydro-glucose units in CNC. In another article, a giant dipole moment was measured in CNC and indirectly linked to possible piezoelectric effects.^[197] Despite these two descriptions, literature data provides extremely broadly and sparse values for CNC piezo constant and a recent article questions the real nature of the measured piezoelectric effect in CNC materials, proposing an explanation of the broad and scattered data about the piezoelectric coefficient in CNC as originating from different electromechanical coupled effects (such as ion migration, flexoelectricity, electrostriction, etc.) so that the d_{33} component of the piezoelectric coefficient varies of about three orders of magnitude from 100 to 10^3 pc/N.^[198]

5.4. Structural Colors

Self-assembly of CNCs is a widely reported phenomenon in literature. The possibility of colloids to self-arrange into period structures behaving as diffractive elements is a phenomenon reported since long time and nature provide striking examples of bright colors in animals and plants due to the controlled arrangement of structural elements. The optical properties of these materials are well known and, in essence, their structure satisfies the Bragg condition (see Equation (2)):

$$m \cdot \frac{\lambda}{n_{\text{eff}}} = p \cdot \cos\theta \quad (2)$$

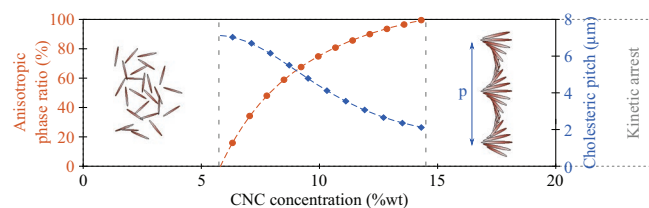


Figure 14. Schematic of the self-assembly of a CNC suspension upon evaporation to form a structurally colored film. The phase diagram shows the transition from isotropic, at low CNC concentration to cholesteric phase at high CNC concentration. Orange circles sketch the amount of menematic phase upon increasing CNC concentration, while the blue diamonds indicate the corresponding equilibrium pitch. Adapted under the terms of the CC-BY 4.0 license.^[158] Copyright 2017, The Authors, published by Wiley-VCH.

where m is the diffraction order, λ is the wavelength in vacuum, n_{eff} is the effective refractive index, and p is the pitch of the helix. Since the director is invariant upon inversion ($\vec{n} = -\vec{n}$), only half-pitch accounts for the system periodicity. θ is the angle of incidence defined to the normal to the interface. **Figure 14a** shows how the isotropic-to-nematic phase transition passes through a biphasic regime where both isotropic and tactoid domains are present. At the highest CNC concentration, nematic domains appear, followed by the kinetic arrest when not enough liquid is present to allow for re-orientation of the colloids/tactoids. CNCs display the typical isotropic-to-nematic phase transition of colloids, and this phenomena has been reviewed several times, even recently in dedicated publications.^[72,158,199] The formation of large domains of nematic phase in CNC colloidal suspensions is a complex process in which different space and time scales interact. The isotropic-to-nematic phase transition couples kinetic and thermodynamic aspects, recently investigated with the help of numerical simulations^[200,201] and confirming the main results of the Onsager theory.^[202] The I-to-N phase transition might be either a 1st order one or a spinodal decomposition, depending on the particle aspect ratio and on the suspension supersaturation (smaller values of these two parameters favor the latter one). Moreover, experimental results demonstrate that the size of the nematic domains depends also on the equilibration of the CNC suspension for extremely long times (several days, being a time scale much longer than those considered in numerical simulations) before starting the EISA deposition.^[203] Experimental details of how the CNC suspension is poured into the container and edge effects might have a predominant role in the formation of interference colors that might or might not be related to nematic phases. For example, the rainbow color that appeared after EISA toward the edge of the Petri dish used as container might correlate either with linear birefringence or film thickness variation.^[204] Some recent articles investigate the formation of CNC tactoids and their internal structure, showing complex dynamics of formation and the coexistence of multiple structures within the same CNC droplet.^[205,206] Recently, the use of vacuum-assisted self-assembly demonstrates important advantage over the EISA one and poses some questions about the dynamics of formation of the nematic phase.^[207] In fact, the authors demonstrate that the flow induced by vacuum suction helps the formation of a highly

ordered nematic phase. The advantages of the VASA method are at least twice: 1) the time required to form the nematic film is reduced by at least an order of magnitude (not considering the several days long equilibration time of the solutions used in EISA), 2) the flow induced by the vacuum suction force the tactoids to reorient and to form helices with their axis parallel to the flow direction. As suggested by the numerical simulations, tactoids form as soon as the CNC solution becomes supersaturated; thus, the higher CNC concentration near the surface of the filter paper stimulates the formation of a large number of randomly oriented tactoids. Since the entire volume of the already deposited CNC is kept wet during the filtration, tactoids are free to re-orient and to form centimeter-sized and structurally homogeneous CNC iridescent nematic domains.^[208,209] On the other hand, during EISA, there is no driving force to orient the tactoids and, while the liquid evaporates from the drop, they might freeze at the critical concentration maintaining their random orientation.

5.5. Back to Wood: Nanocellulose Films by Delignification

Nanocellulose is not just a versatile nanomaterial, it is a biological molecule synthesized in nature in various plants or bacteria, in particular as a fundamental component of xylem. Xylem is made of a network of load-bearing fibers that provides mechanical support, strength, rigidity, and the main mechanisms for transporting water and nutrients from plant's root to shoots.^[210] Although the molecular architecture of the xylem is complex and variable among different plants, in general, it consists of elementary cellulose (CNF with crystalline regions) coated by hemicellulose to form microfibrils (shown in Figure 1), the exact structure of which is still a matter of research. Xylan and galactoglucomannan (GGM) are the principal hemicelluloses in hardwood and softwood; they bind to the hydrophilic and hydrophobic surface of cellulose^[211] and assemble into larger order structures, that is the macrofibrils. Hydrogen bond networks exist between the cellulose and the lignin, as well as the cellulose and the hemicellulose, although covalent linkages have also been proposed to be present between the cellulose and the lignin.^[212] A model of the macrofibrils of softwood is shown in **Figure 15**.

The hierarchical bottom-up architecture (from CNF to macrofibrils) is intrinsically anisotropic, being all the molecules and fibrils more or less aligned along with the wood structure. An innovative approach emerging in the last years is to pass from wood to NC films directly, tailoring and functionalizing the hierarchical nanostructure of bulk wood to obtain functional materials.^[214] By this approach, it is possible to skip many of the steps necessary to extract bulk cellulose, scale down its dimension up to the nanosize and fabricate free-standing films of nanowood.^[215] Apart from the saving of resources and reagents and the reduction of wastes, the intrinsic wood architecture is retained in the wood films, so that the strongly anisotropic physical properties of individual CNF are not averaged out. A well-established chemical treatment (i.e., boiling in a sodium hydroxide/sodium sulfite solution) is the simplest procedure to transform bulk natural wood directly into a high-performance structural densified material with highly

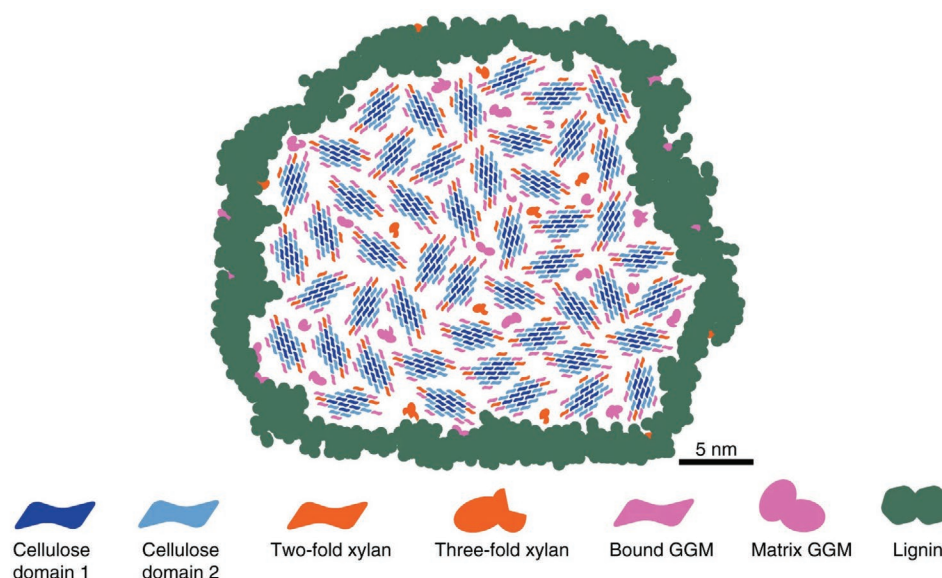


Figure 15. Model of molecular architecture of softwood. The model was obtained on the bases of solid state NMR. Domain 1 and domain 2 were distinguishable on the basis of chemical shift values and belong to different cellulose conformations. It has been proposed that domain 1 cellulose occurs on the cellulose hydrophilic surfaces when bound to xylan. Hydrophobic surface glucosyl residues in domain 2 are bound by hemicelluloses through interactions mostly other than hydrogen bonding. Adapted under the terms of the CC-BY 4.0 license.^[213] Copyright 2019, The Authors, published by Springer Nature.

aligned cellulose nanofibers.^[216] Thin, transparent films with outstanding anisotropic properties have been obtained by performing, first delignification in a NaClO aqueous solution and then mechanical pressing, as shown in **Figure 16**. These films can guide liquid transport, allow for anisotropic effects in light transmittance, and possess enhanced mechanical properties.^[217]

An anisotropic paper material possessing high mechanical flexibility and outstanding optical properties with both high transmittance ($\approx 90\%$) and high haze ($\approx 90\%$) was obtained by shear pressing Basswood slices delignified with a NaClO solution.^[218] The shear pressing forces the wood fibers to one direction which results in an anisotropic structure with low refractive index fluctuations in the direction of the aligned cellulose fibers. Conversely, if vertical pressing is applied to the delignified radial wood, isotropic transparent paper with randomly distributed cellulose fibers is obtained. Breathable porous thin films nanowood have been obtained for skin-interfaced electronics, where “sensitive” biosensing (transporting sweat), “insulation” between units, and “targeted” delivery of saline-soluble drugs are necessary.^[219]

The films obtained from wood require simple, environmentally friendly, and cost-effective fabrication methods. Depending on the method details, the film characteristics (i.e., anisotropy, transparency, flexibility) can be appropriately tuned. This approach offers advantageous opportunities for fabricating low-cost films and transparent papers to be used in optical and electronic devices and in solar cells.^[220] Besides the sophisticated applications in the construction industry, in solar cells, and in electronics, nanowood opens new perspectives in membrane science and water remediation. The array of cellulose nanofibers that are exposed after extraction of intertwined lignin and hemicellulose from the natural wood are separated by aligned nanochannels. In this regard, films from wood are

a nanoporous material, which allows the transport of fluids. Membranes and fluidic devices with highly efficient and tunable ion regulation have been obtained by delignified wood.^[221] By applying the cellulose modification routes, the nanochannels have been lined with charged surface functional groups which attract layers of counter ions adjacent to the nanofibers. The surface effects (i.e., interface electrostatic interactions) of the nanochannels governed ion transport along the fiber direction, enabling ionic separation and a tunable ionic conductivity. Thanks to porous structure and CNC alignment, nanowood behaves as a “guiding biofilm” suitable for directional heat and sweat transport. These are some of the desired features for on-skin electronics that offers new and sophisticated applications for this conceptually simple but amazing nanomaterial. This concept is summarized in **Figure 17**. **Figure 17** (panel a) shows the schematic drawing of a typical softwood (*Pinus sylvestris* var. *mongolica* Litv) where CNCs grow along different directions in various layers (L1–L3) but are well-aligned along the wood growth direction in the L2 layer which occupies the main portion of the cell walls. Shaving wood along its growth direction (making lumens in the plane of the wood slice) in the tangential direction with respect to annual rings (**Figure 17a**) favors higher thermal conductivity in the tangential direction, due to the influence of radially oriented wood rays. If lignin is removed and then solvent exchange and gentle drying is performed, a porous delignified biofilm is obtained, with high transport in the CNC direction, since inter CNCs pores are produced while CNC alignment is preserved (**Figure 17b**). If a compression is applied after delignification, a transparent biofilm is obtained, with a densified CNC arrangement (**Figure 17c**). This more packed structure guarantees adequate cross-plane breathability and sweat guiding along the CNC direction.

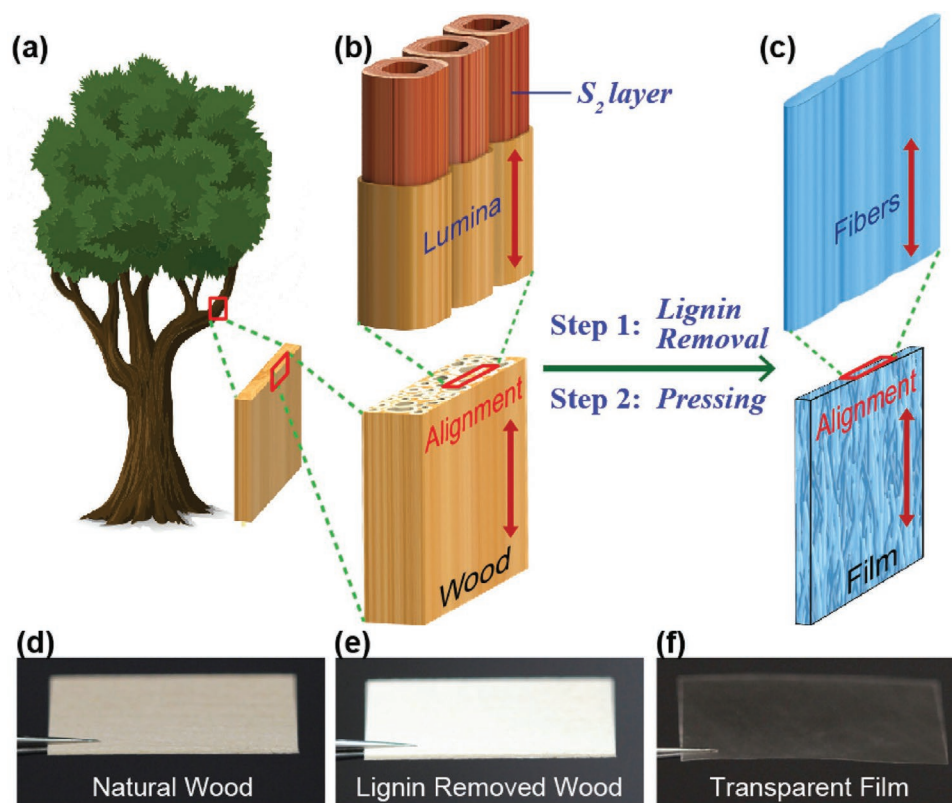


Figure 16. Schematics of direct transformation of an anisotropic wood slice into an anisotropic transparent film by lignin removal and mechanical pressing. a) Wood microstructures. b) The two-step fabrication process. Step 1: Lignin removal. Step 2: Mechanical pressing. c) The lumina are fully closed after mechanical pressing. During Step 1 and Step 2, both the microscale alignment for lumen and the nanoscale alignment for CNFs in natural wood are well preserved in the resulting transparent film. d–f) Photos of the color changes from yellow natural wood (d) to white wood (e) and finally to a transparent film (f). Reproduced with permission.^[217] Copyright 2017, Wiley-VCH.

Hydrophobic nanowood membranes characterized by high porosity and hierarchical pore structure have been fabricated for water desalination. The membranes were characterized by a wide pore size distribution of crystalline cellulose nanofibrils, xylem vessels, and lumina channels. The intrinsic permeability of the porous structure allowed high water vapor transport while the high thermal conductivity along the fibers enabled efficient thermal dissipation along the axial direction. Conversely, the thermal conductivity of the nanowood was extremely low in the transverse direction, which reduced conductive heat transport. As a result, the membrane demonstrated excellent intrinsic vapor permeability and thermal efficiency.^[222] A mesoporous 3D wood membrane decorated with Pd nanoparticles was proved to function as an excellent waste water treatment material, thanks to the synergistic effect of the evenly distributed nanosized catalyst particles and the channel structure of the hardwood.^[223] Filling the network of channels of nanowood with different molecules or nanostructures is a simple approach for manufacturing composite materials. Indeed, impregnation with polyethylene,^[224] spin-assisted LbL deposition of poly(vinyl amine),^[225] or filling with nanoparticles of silicon carbide and graphene oxide,^[226] resulted in materials with superior performances, such as mechanical anisotropic resistance, hindered water uptake and chemical oxidation,^[224] tensile strength exceeding that of the

original tree,^[225] increased fire-retarding, and thermo-indentation resistances.^[226]

6. Conclusion

The exceptional properties of NC are the heritage of the natural vegetable or bacterial from which NC is produced. These biological sources dictate the NC structure and behavior, for better or worse.

The only possibility of manipulating the NC properties are provided by the interface chemical groups (i.e., the hydroxyls or, at a lower extent, the groups introduced by the cellulose degradation procedures), as shown by the examples of NC applications described in this review.

There are still partially unresolved problems to engineer the NC's assembly and the NC's film interface properties.

An interesting possibility to change physical properties and chemical reactivity is provided by the fringing of the compact CNC or CNF structure, which increases the accessible surface area and exposes the internal glucose residues.

Several procedures can be applied to tailor the interface. The procedures performed in the bulk solutions are often limited by the low solubility of NC in organic apolar solvents. Ionic liquids could offer interesting opportunities, but these are still little

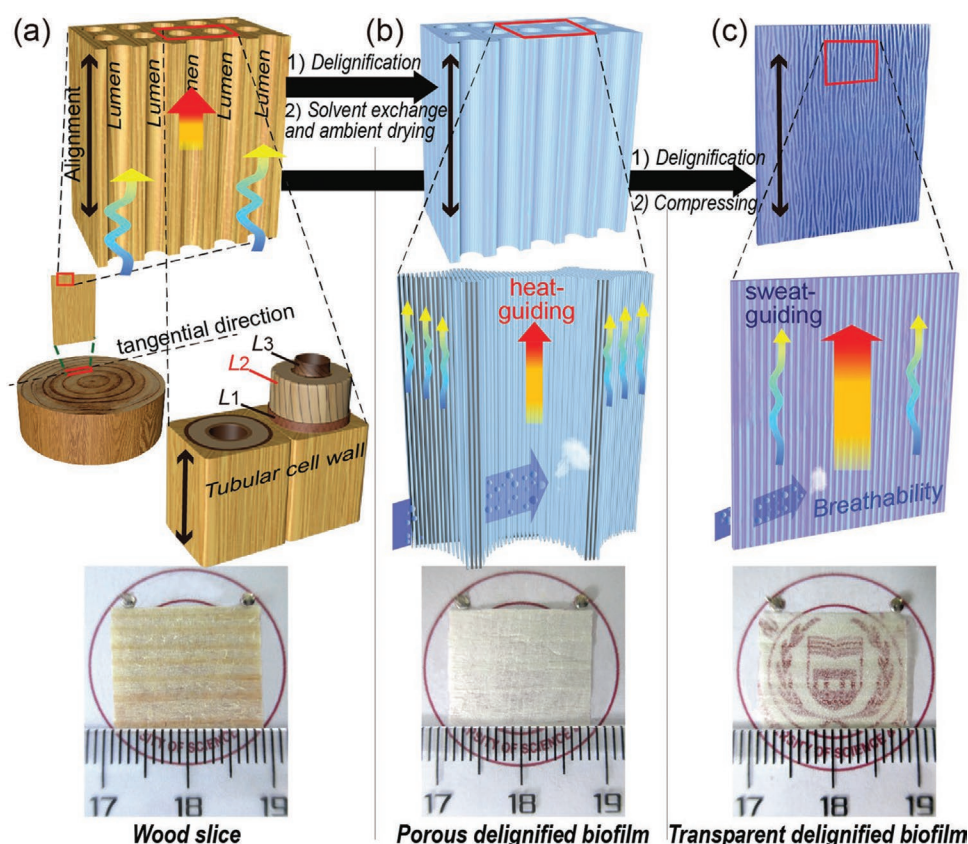


Figure 17. Schematics of the fabrication of breathable nanowood biofilms: the well-aligned CNs in L2 layer (the main portion of the cell walls) of a) wood slice is transferred into the porous delignified biofilm (b) and transparent delignified biofilm (c). Adapted with permission.^[219] Copyright 2019, Wiley-VCH.

explored. The use of enzymes in aqueous solutions is the other future possibility.

Gas-phase tailoring of the interface is a strongly promising approach, in particular to modify the films' surface. By this approach, the one side modification of the films or their patterning is also possible. The alternative approach is based on the conservation of NC coating of hemicellulose. It offers several advantages: The procedure causes less pollution, then, the colloidal stability, and probably, the reactivity of the hydroxyls are increased, thanks to the soft hemicellulose coating.

The emerging applications of NCs are going beyond the hydrogels, aerogels, and films. The perspective is to obtain ordered materials, layered structures, aligned CNC or CNF bundles, regular porous networks and self-orienting interfaces. With the advent of the 3D printing technologies, we can expect that in a short time physical NC objects will be available, characterized by a precise control of the structure at macroscopic and microscopic level, obtained by the computer aided design, the tuning of the composition of the extruded fluid, and the use of a nozzle which orient the fibers. The main issue for the widespread implementation of the NC production is the environmental impact. Despite that NC is often considered "environmental friendly," its synthesis requires aggressive chemicals and an elevated energy cost. Wood films have a lower environmental impact and could find several applications, even though not as much as CNC and CNF.

Acknowledgements

This activity has received funding from the MIUR under the project PRIN PANACEA (2017LEPH3M); CUP E64I190001150001.349.

Open access funding provided by Università degli Studi di Trento within the CRUI-CARE Agreement.

Conflict of Interest

The authors declare no conflict of interest.

Keywords

colloids, nanocellulose interface, nematic phase in cellulose nanocrystals colloidal suspensions, Pickering emulsions

Received: August 24, 2021

Revised: November 2, 2021

Published online: December 29, 2021

- [1] R. M. Erb, J. S. Sander, R. Grisch, A. R. Studart, *Nat Commun* **2013**, 4, 1712.
- [2] F. G. Torres, J. J. Arroyo, O. P. Troncoso, *Mater. Sci. Eng., C* **2019**, 98, 1277.
- [3] A. Dufresne, *Mater. Today* **2013**, 16, 220.

- [4] T. Saito, Y. Nishiyama, J.-L. Putaux, M. Vignon, A. Isogai, *Biomacromolecules* **2006**, *7*, 1687.
- [5] A. Barhoum, P. Samyn, T. Öhlund, A. Dufresne, *Nanoscale* **2017**, *9*, 15181.
- [6] M. Wakabayashi, S. Fujisawa, T. Saito, A. Isogai, *Front. Chem.* **2020**, *8*, 37.
- [7] K. J. De France, T. Hoare, E. D. Cranston, *Chem. Mater.* **2017**, *29*, 4609.
- [8] L. Wågberg, J. Erlandsson, *Adv. Mater.* **2021**, *33*, 2001474.
- [9] Y. Habibi, *Chem. Soc. Rev.* **2014**, *43*, 1519.
- [10] X. Yang, S. K. Biswas, J. Han, S. Tanpichai, M.-C. Li, C. Chen, S. Zhu, A. K. Das, H. Yano, *Adv. Mater.* **2021**, *33*, 2002264.
- [11] S. Sinquefeld, P. N. Ciesielski, K. Li, D. J. Gardner, S. Ozcan, *ACS Sustainable Chem. Eng.* **2020**, *8*, 9601.
- [12] K. Heise, E. Kontturi, Y. Allahverdiyeva, T. Tammelin, M. B. Linder, Nonappa, O. Ikkala, *Adv. Mater.* **2021**, *33*, 2004349.
- [13] F. Hoeng, A. Denneulin, J. Bras, *Nanoscale* **2016**, *8*, 13131.
- [14] L. J. Gibson, *J. R. Soc. Interface* **2012**, *9*, 2749.
- [15] A. C. O'Sullivan, *Cellulose* **1997**, *4*, 173.
- [16] T. Wuestenberg, *Cellulose and Cellulose Derivatives in the Food Industry: Fundamentals and Applications*, Wiley, New York **2014**.
- [17] Z. Peter, *Carbohydr. Polym.* **2021**, *254*, 117417.
- [18] S. Pérez, D. Samain, in *Advances in Carbohydrate Chemistry and Biochemistry* (Ed: D. Horton), vol. 64, Academic Press, San Diego, CA **2010**, pp. 25–116.
- [19] A. Dufresne, *Nanocellulose: From Nature to High Performance Tailored Materials*, De Gruyter, Berlin **2012**.
- [20] C. Djahedi, L. A. Berglund, J. Wohler, *Carbohydr. Polym.* **2015**, *130*, 175.
- [21] F. L. Dri, L. G. Hector, R. J. Moon, P. D. Zavattieri, *Cellulose* **2013**, *20*, 2703.
- [22] I. Diddens, B. Murphy, M. Krisch, M. Müller, *Macromolecules* **2008**, *41*, 9755.
- [23] H. Wang, D. Li, H. Yano, K. Abe, *Cellulose* **2014**, *21*, 1505.
- [24] Y. Yue, C. Zhou, A. D. French, G. Xia, G. Han, Q. Wang, Q. Wu, *Cellulose* **2012**, *19*, 1173.
- [25] B. Medronho, B. Lindman, *Curr. Opin. Colloid Interface Sci.* **2014**, *19*, 32.
- [26] F. Jiang, Y.-L. Hsieh, *ACS Sustainable Chem. Eng.* **2016**, *4*, 1041.
- [27] L.-S. Johansson, T. Tammelin, J. M. Campbell, H. Setälä, M. Österberg, *Soft Matter* **2011**, *7*, 10917.
- [28] D. M. Rein, R. Khalfin, Y. Cohen, *J. Colloid Interface Sci.* **2012**, *386*, 456.
- [29] I. Capron, O. J. Rojas, R. Bordes, *Curr. Opin. Colloid Interface Sci.* **2017**, *29*, 83.
- [30] C. Bruel, S. Queffulou, P. J. Carreau, J. R. Tavares, M.-C. Heuzey, *Langmuir* **2020**, *36*, 12179.
- [31] A. Isogai, *Adv. Mater.* **2021**, *33*, 2000630.
- [32] Y. Nishiyama, U.-J. Kim, D.-Y. Kim, K. S. Katsumata, R. P. May, P. Langan, *Biomacromolecules* **2003**, *4*, 1013.
- [33] T. Saito, A. Isogai, *Biomacromolecules* **2004**, *5*, 1983.
- [34] C. Zhang, S. Ketten, D. Derome, J. Carmeliet, *Carbohydr. Polym.* **2021**, *258*, 117682.
- [35] Y. Hou, Q.-F. Guan, J. Xia, Z.-C. Ling, Z. He, Z.-M. Han, H.-B. Yang, P. Gu, Y. Zhu, S.-H. Yu, H. Wu, *ACS Nano* **2021**, *15*, 1310.
- [36] A. Y. Mehandzhyski, N. Rolland, M. Garg, J. Wohler, M. Linares, I. Zozoulenko, *Cellulose* **2020**, *27*, 4221.
- [37] Z. Li, W. Xia, *Extreme Mech. Lett.* **2020**, *40*, 100942.
- [38] A. H. Tayeb, E. Amini, S. Ghasemi, M. Tajvidi, *Molecules* **2018**, *23*, 2684.
- [39] F. J. Martin-Martinez, *PNAS* **2018**, *115*, 7174.
- [40] Y. Nishiyama, *Philosophical Transactions of the Royal Society A: Mathematical, Physical and Engineering Sciences* **2018**, *376*, 20170047.
- [41] C. Bruel, J. R. Tavares, P. J. Carreau, M.-C. Heuzey, *Carbohydr. Polym.* **2019**, *205*, 184.
- [42] Y. Nishiyama, G. P. Johnson, A. D. French, *Cellulose* **2012**, *19*, 319.
- [43] E. Niinivaara, M. Faustini, T. Tammelin, E. Kontturi, *Langmuir* **2015**, *31*, 12170.
- [44] U. Weise, T. Maloney, H. Paulapuro, *Cellulose* **1996**, *3*, 189.
- [45] M. Pääkkö, M. Ankerfors, H. Kosonen, A. Nykänen, S. Ahola, M. Österberg, J. Ruokolainen, J. Laine, P. T. Larsson, O. Ikkala, T. Lindström, *Biomacromolecules* **2007**, *8*, 1934.
- [46] C. A. Maestri, M. Abrami, S. Hazan, E. Chisté, Y. Golan, J. Rohrer, A. Bernkop-Schnürch, M. Grassi, M. Scarpa, P. Bettotti, *Sci Rep* **2017**, *7*, 11129.
- [47] N. Ferrari, C. A. Maestri, P. Bettotti, M. Grassi, M. Abrami, M. Scarpa, *Molecules* **2021**, *26*, 2552.
- [48] E. G. Facchine, R. J. Spontak, O. J. Rojas, S. A. Khan, *Biomacromolecules* **2020**, *21*, 3561.
- [49] Y. Xu, A. D. Atrens, J. R. Stokes, *Soft Matter* **2018**, *14*, 1953.
- [50] L. Mendoza, T. Gunawardhana, W. Batchelor, G. Garnier, *J. Colloid Interface Sci.* **2018**, *525*, 119.
- [51] C. Salas, T. Nypelö, C. Rodríguez-Abreu, C. Carrillo, O. J. Rojas, *Curr. Opin. Colloid Interface Sci.* **2014**, *19*, 383.
- [52] B. Medronho, A. Romano, M. G. Miguel, L. Stigsson, B. Lindman, *Cellulose* **2012**, *19*, 581.
- [53] O. Biermann, E. Hädicke, S. Koltzenburg, F. Müller-Plathe, *Angew. Chem. Int. Ed.* **2001**, *40*, 3822.
- [54] L. E. Silva, A. d. A. dos Santos, L. Torres, Z. McCaffrey, A. Klamczynski, G. Glenn, A. R. d. Sena Neto, D. Wood, T. Williams, W. Orts, R. A. P. Damásio, G. H. D. Tonoli, *Carbohydr. Polym.* **2021**, *252*, 117165.
- [55] U. P. Agarwal, S. A. Ralph, R. S. Reiner, C. Baez, *Cellulose* **2016**, *23*, 125.
- [56] M. Wang, X. Tian, R. H. A. Ras, O. Ikkala, *Adv. Mater. Interfaces* **2015**, *2*, 1500080.
- [57] P. Bettotti, C. A. Maestri, R. Guider, I. Mancini, E. Nativ-Roth, Y. Golan, M. Scarpa, *Adv. Mater. Interfaces* **2016**, *3*, 1500415.
- [58] B. P. Binks, *Curr. Opin. Colloid Interface Sci.* **2002**, *7*, 21.
- [59] T. Saito, M. Hirota, N. Tamura, S. Kimura, H. Fukuzumi, L. Heux, A. Isogai, *Biomacromolecules* **2009**, *10*, 1992.
- [60] S. Fujisawa, Y. Okita, H. Fukuzumi, T. Saito, A. Isogai, *Carbohydr. Polym.* **2011**, *84*, 579.
- [61] C. A. Maestri, A. Motta, L. Moschini, A. Bernkop-Schnürch, R. A. Baus, P. Lecca, M. Scarpa, *J. Biomed. Mater. Res. Part A* **2020**, *108*, 1509.
- [62] G. Pangu, E. Johnston, J. Petkov, N. Parry, M. Leach, D. A. Hammer, *Langmuir* **2007**, *23*, 10682.
- [63] E. D. Cranston, D. G. Gray, *Colloids Surf. A* **2008**, *325*, 44.
- [64] C. Aulin, S. Ahola, P. Josefsson, T. Nishino, Y. Hirose, M. Österberg, L. Wågberg, *Langmuir* **2009**, *25*, 7675.
- [65] G. Decher, *Science* **1997**, *277*, 1232.
- [66] M. Ghanadpour, F. Carosio, L. Wågberg, *Appl. Mater. Today* **2017**, *9*, 229.
- [67] K. Shanmugam, S. Varanasi, G. Garnier, W. Batchelor, *Cellulose* **2017**, *24*, 2669.
- [68] D. Beneventi, D. Chaussy, D. Curtin, L. Zolin, C. Gerbaldi, N. Penazzi, *Ind. Eng. Chem. Res.* **2014**, *53*, 10982.
- [69] Y.-T. Li, S.-B. Lin, L.-C. Chen, H.-H. Chen, *Cellulose* **2017**, *24*, 4871.
- [70] W. Ohm, A. Rothkirch, P. Pandit, V. Köstgens, P. Müller-Buschbaum, R. Rojas, S. Yu, C. J. Brett, D. L. Söderberg, S. V. Roth, *J. Coat. Technol. Res.* **2018**, *15*, 759.
- [71] A. Sydney Gladman, E. A. Matsumoto, R. G. Nuzzo, L. Mahadevan, J. A. Lewis, *Nat. Mater.* **2016**, *15*, 413.
- [72] K. De France, Z. Zeng, T. Wu, G. Nyström, *Adv. Mater.* **2021**, *33*, 2000657.
- [73] L. Y. Ee, S. F. Y. Li, *Nanoscale Adv.* **2021**, *3*, 1167.
- [74] X. Wang, Q. Wang, C. Xu, *Bioengineering* **2020**, *7*, 40.
- [75] S. Sultan, G. Siqueira, T. Zimmermann, A. P. Mathew, *Curr. Opin. Biomed. Eng.* **2017**, *2*, 29.

- [76] G. Siqueira, D. Kokkinis, R. Libanori, M. K. Hausmann, A. S. Gladman, A. Neels, P. Tingaut, T. Zimmermann, J. A. Lewis, A. R. Studart, *Adv. Functional Materials* **2017**, 27, 1604619.
- [77] M. K. Hausmann, G. Siqueira, R. Libanori, D. Kokkinis, A. Neels, T. Zimmermann, A. R. Studart, *Adv. Funct. Mater.* **2020**, 30, 1904127.
- [78] M. Hubbe, A. Ferrer, P. Tyagi, Y. Yin, C. Salas, L. Pal, O. Rojas, *BioResources* **2017**, 12, 2143.
- [79] M. Matsumoto, T. Kitaoka, *Adv. Mater.* **2016**, 28, 1765.
- [80] D. Roilo, C. A. Maestri, M. Scarpa, P. Bettotti, W. Egger, T. Koschine, R. S. Brusa, R. Checchetto, *J. Phys. Chem. C* **2017**, 121, 15437.
- [81] L. Ansaloni, J. Salas-Gay, S. Ligi, M. G. Baschetti, *J. Membr. Sci.* **2017**, 522, 216.
- [82] L. Wang, C. Chen, J. Wang, D. J. Gardner, M. Tajvidi, *Food Packag. Shelf Life* **2020**, 23, 100464.
- [83] S. Belbekhouche, J. Bras, G. Siqueira, C. Chappey, L. Lebrun, B. Khelifi, S. Marais, A. Dufresne, *Carbohydr. Polym.* **2011**, 83, 1740.
- [84] H. Fukuzumi, T. Saito, T. Iwata, Y. Kumamoto, A. Isogai, *Biomacromolecules* **2009**, 10, 162.
- [85] H. Fukuzumi, T. Saito, S. Iwamoto, Y. Kumamoto, T. Ohdaira, R. Suzuki, A. Isogai, *Biomacromolecules* **2011**, 12, 4057.
- [86] C. J. Brett, N. Mittal, W. Ohm, M. Gensch, L. P. Kreuzer, V. Köstgens, M. Månsson, H. Frielinghaus, P. Müller-Buschbaum, L. D. Söderberg, S. V. Roth, *Macromolecules* **2019**, 52, 4721.
- [87] R. A. Chowdhury, M. Nuruddin, C. Clarkson, F. Montes, J. Howarter, J. P. Youngblood, *ACS Appl. Mater. Interfaces* **2019**, 11, 1376.
- [88] C. Aulin, E. Karabulut, A. Tran, L. Wågberg, T. Lindström, *ACS Appl. Mater. Interfaces* **2013**, 5, 7352.
- [89] J. Vartiainen, K. Rose, Y. Kusano, J. Mannila, L. Wikström, *J. Coat. Technol. Res.* **2020**, 17, 305.
- [90] P. Willberg-Keyriläinen, J. Vartiainen, J. Pelto, J. Ropponen, *Carbohydr. Polym.* **2017**, 170, 160.
- [91] S. S. Nair, H. Chen, Y. Peng, Y. Huang, N. Yan, *ACS Sustainable Chem. Eng.* **2018**, 6, 10058.
- [92] G. Pilon, J.-M. Lavoie, *ACS Sustainable Chem. Eng.* **2013**, 1, 198.
- [93] K.-M. Chin, S. S. Ting, H. L. Ong, M. Omar, *J. Appl. Polymer Science* **2018**, 135, 46065.
- [94] V. Thakur, A. Guleria, S. Kumar, S. Sharma, K. Singh, *Mater. Adv.* **2021**, 2, 1872.
- [95] H. Abushammala, J. Mao, *Molecules* **2019**, 24, 2782.
- [96] B. Thomas, M. C. Raj, A. K. B. R. M. H. J. Joy, A. Moores, G. L. Drisko, C. Sanchez, *Chem. Rev.* **2018**, 118, 11575.
- [97] F. Jiang, J. L. Dallas, B. K. Ahn, Y.-L. Hsieh, *Carbohydr. Polym.* **2014**, 110, 360.
- [98] Y. Okita, T. Saito, A. Isogai, *Biomacromolecules* **2010**, 11, 1696.
- [99] R. Koshani, T. G. M. van de Ven, *J. Colloid Interface Sci.* **2020**, 563, 252.
- [100] H. Tao, N. Lavoine, F. Jiang, J. Tang, N. Lin, *Nanoscale Horiz.* **2020**, 5, 607.
- [101] K. Heise, T. Koso, L. Pitkänen, A. Potthast, A. W. T. King, M. A. Kostiaainen, E. Kontturi, *ACS Macro Lett.* **2019**, 8, 1642.
- [102] K. Heise, G. Delepierre, A. W. T. King, M. A. Kostiaainen, J. Zoppe, C. Weder, E. Kontturi, *Angew. Chem. Int. Ed.* **2021**, 60, 66.
- [103] A. R. Lokanathan, A. Nykänen, J. Seitonen, L.-S. Johansson, J. Campbell, O. J. Rojas, O. Ikkala, J. Laine, *Biomacromolecules* **2013**, 14, 2807.
- [104] A. Ferguson, U. Khan, M. Walsh, K.-Y. Lee, A. Bismarck, M. S. P. Shaffer, J. N. Coleman, S. D. Bergin, *Biomacromolecules* **2016**, 17, 1845.
- [105] M. A. S. Azizi Samir, F. Alloin, J.-Y. Sanchez, N. El Kissi, A. Dufresne, *Macromolecules* **2004**, 37, 1386.
- [106] M. A. S. Azizi Samir, F. Alloin, A. Dufresne, *Biomacromolecules* **2005**, 6, 612.
- [107] D. Viet, S. Beck-Candanedo, D. G. Gray, *Cellulose* **2007**, 14, 109.
- [108] G. Siqueira, J. Bras, A. Dufresne, *Biomacromolecules* **2009**, 10, 425.
- [109] Y. Okita, S. Fujisawa, T. Saito, A. Isogai, *Biomacromolecules* **2011**, 12, 518.
- [110] A. Salama, P. Hesemann, *ACS Sustainable Chem. Eng.* **2020**, 8, 17893.
- [111] Y. Li, J. Wang, X. Liu, S. Zhang, *Chem. Sci.* **2018**, 9, 4027.
- [112] J. H. Jordan, M. W. Easson, B. D. Condon, *RSC Adv.* **2020**, 10, 39413.
- [113] G. A. S. Haron, H. Mahmood, M. H. Noh, M. Z. Alam, M. Moniruzzaman, *ACS Sustainable Chem. Eng.* **2021**, 9, 1008.
- [114] Z. Man, N. Muhammad, A. Sarwono, M. A. Bustam, M. Vignesh Kumar, S. Rafiq, *J. Polym. Environ.* **2011**, 19, 726.
- [115] E. E. Jaekel, J. A. Sirviö, M. Antonietti, S. Filonenko, *Green Chem.* **2021**, 23, 2317.
- [116] F. Huang, X. Wu, Y. Yu, Y. Lu, Q. Chen, *Carbohydr. Polym.* **2017**, 155, 525.
- [117] S. Yang, Q. Xie, X. Liu, M. Wu, S. Wang, X. Song, *RSC Adv.* **2018**, 8, 3619.
- [118] Y. Wang, X. Wang, Y. Xie, K. Zhang, *Cellulose* **2018**, 25, 3703.
- [119] K. Pacaphol, D. Aht-Ong, *Surf. Coat. Technol.* **2017**, 320, 70.
- [120] M. Li, X. Li, X. An, Z. Chen, H. Xiao, *Front. Chem.* **2019**, 7, 447.
- [121] M. Ghasemlou, F. Daver, E. P. Ivanova, Y. Habibi, B. Adhikari, *Prog. Polym. Sci.* **2021**, 119, 101418.
- [122] C. E. Hoyle, C. N. Bowman, *Angew. Chem. Int. Ed.* **2010**, 49, 1540.
- [123] A. Fatona, R. M. Berry, M. A. Brook, J. M. Moran-Mirabal, *Chem. Mater.* **2018**, 30, 2424.
- [124] J. Guo, W. Fang, A. Welle, W. Feng, I. Filpponen, O. J. Rojas, P. A. Levkin, *ACS Appl. Mater. Interfaces* **2016**, 8, 34115.
- [125] J. Guo, I. Filpponen, L.-S. Johansson, S. Heissler, L. Li, P. Levkin, O. J. Rojas, *Cellulose* **2018**, 25, 367.
- [126] Y. Wang, Z. Qiu, Z. Lang, Y. Xie, Z. Xiao, H. Wang, D. Liang, J. Li, K. Zhang, *Adv. Mater.* **2021**, 33, 2005263.
- [127] G. Chinga-Carrasco, N. Kuznetsova, M. Garaeva, I. Leirset, G. Galiullina, A. Kostochko, K. Syverud, *J. Nanopart. Res.* **2012**, 14, 1280.
- [128] C. N. Flynn, C. P. Byrne, B. J. Meenan, *Surf. Coat. Technol.* **2013**, 233, 108.
- [129] S. Prabhu, K. Vaideki, S. Anitha, *Carbohydr. Polym.* **2017**, 156, 34.
- [130] D. M. Panaitescu, E. R. Ionita, C.-A. Nicolae, A. R. Gabor, M. D. Ionita, R. Trusca, B.-E. Lixandru, I. Codita, G. Dinescu, *Polymers* **2018**, 10, 1249.
- [131] S. Vizireanu, D. M. Panaitescu, C. A. Nicolae, A. N. Frone, I. Chiulan, M. D. Ionita, V. Satulu, L. G. Carpen, S. Petrescu, R. Birjega, G. Dinescu, *Sci Rep* **2018**, 8, 15473.
- [132] D. M. Panaitescu, S. Vizireanu, C. A. Nicolae, A. N. Frone, A. Casarica, L. G. Carpen, G. Dinescu, *Nanomaterials* **2018**, 8, 467.
- [133] T. Nypelö, H. Amer, J. Konnerth, A. Potthast, T. Rosenau, *Biomacromolecules* **2018**, 19, 973.
- [134] S. Afrin, Z. Karim, *ChemBioEng Reviews* **2017**, 4, 289.
- [135] V. Arantes, I. K. R. Dias, G. L. Berto, B. Pereira, B. S. Marotti, C. F. O. Nogueira, *Cellulose* **2020**, 27, 10571.
- [136] E. Aracri, T. Vidal, A. J. Ragauskas, *Carbohydr. Polym.* **2011**, 84, 1384.
- [137] A. G. Morena, M. B. Roncero, S. V. Valenzuela, C. Valls, T. Vidal, F. I. J. Pastor, P. Diaz, J. Martínez, *Cellulose* **2019**, 26, 8655.
- [138] X. Yang, M. S. Reid, P. Olsén, L. A. Berglund, *ACS Nano* **2020**, 14, 724.
- [139] X. Y. Liu, *J. Chem. Phys.* **2000**, 112, 9949.
- [140] H. B. Eral, V. López-Mejías, M. O'Mahony, B. L. Trout, A. S. Myerson, P. S. Doyle, *Cryst. Growth Des.* **2014**, 14, 2073.
- [141] H. K. Hektisch, J. Dennis, J. I. Hanoka, *J. Phys. Chem. Solids* **1965**, 26, 493.
- [142] R. Xiong, H. S. Kim, L. Zhang, V. F. Korolovych, S. Zhang, Y. G. Yingling, V. V. Tsukruk, *Angew. Chem. Int. Ed.* **2018**, 57, 8508.

- [143] N. Rolland, A. Y. Mehandzhyski, M. Garg, M. Linares, I. V. Zozoulenko, *J. Chem. Theory Comput.* **2020**, *16*, 3699.
- [144] C. M. Clarkson, S. M. El Awad Azrak, G. T. Schueneman, J. F. Snyder, J. P. Youngblood, *Polymer* **2020**, *187*, 122101.
- [145] Y. Li, C. Han, Y. Yu, L. Xiao, *Int. J. Biol. Macromol.* **2020**, *147*, 34.
- [146] Q. Lv, C. Xu, D. Wu, Z. Wang, R. Lan, L. Wu, *Composites, Part A* **2017**, *92*, 17.
- [147] A. Clarke, A. A. Vasileiou, M. Kontopoulou, *Poly. Eng. Sci.* **2019**, *59*, 989.
- [148] S. Borysiak, A. Grzabka-Zasadzinska, *J. Appl. Polym. Sci.* **2016**, *133*, 3.
- [149] J. Gao, Q. Li, W. Chen, Y. Liu, H. Yu, *ChemPlusChem* **2014**, *79*, 725.
- [150] P. Kanaujia, P. Poovizhi, W. K. Ng, R. B. H. Tan, *Powder Technol.* **2015**, *285*, 2.
- [151] S. Baghel, H. Cathcart, N. J. O'Reilly, *J. Pharm. Sci.* **2016**, *105*, 2527.
- [152] C. Ruiz-Palomero, S. R. Kennedy, M. L. Soriano, C. D. Jones, M. Valcárcel, J. W. Steed, *Chem. Commun.* **2016**, *52*, 7782.
- [153] M. Banerjee, S. Saraswatula, L. G. Willows, H. Woods, B. Brettmann, *J. Mater. Chem. B* **2018**, *6*, 7317.
- [154] C. Piatto, Ph.D., University of Trento **2019**, <http://eprints-phd.biblio.unitn.it/3575/>.
- [155] C. Yong, C. Mei, M. Guan, Q. Wu, X. Sun, B. Xu, K. Wang, *J. Appl. Polym. Sci.* **2018**, *135*, 45896.
- [156] S. Lombardo, P. Chen, P. A. Larsson, W. Thielemans, J. Wohler, A. J. Svagan, *Langmuir* **2018**, *34*, 5464.
- [157] J. Israelachvili, *Intermolecular and Surface Forces*, Elsevier Science, Oxford **2015**, tex.lccn: 2010031067.
- [158] R. M. Parker, G. Guidetti, C. A. Williams, T. Zhao, A. Narkevicius, S. Vignolini, B. Frka-Petesic, *Adv. Mater.* **2018**, *30*, 1704477.
- [159] Y. Zhu, J. Jiang, K. Liu, Z. Cui, B. P. Binks, *Langmuir* **2015**, *31*, 3301.
- [160] A. G. Cunha, J.-B. Mougel, B. Cathala, L. A. Berglund, I. Capron, *Langmuir* **2014**, *30*, 9327.
- [161] S. Kutuzov, J. He, R. Tangirala, T. Emrick, T. P. Russell, A. Böker, *Phys. Chem. Chem. Phys.* **2007**, *9*, 6351.
- [162] K. R. Peddiredy, T. Nicolai, L. Benyahia, I. Capron, *ACS Macro Lett.* **2016**, *5*, 283.
- [163] C.-Y. Hui, A. Jagota, *Proc. R. Soc. A* **2014**, *470*, 20140085.
- [164] E. R. Jerison, Y. Xu, L. A. Wilen, E. R. Dufresne, *Phys. Rev. Lett.* **2011**, *106*, 186103.
- [165] G. Ahmed, N. Koursari, A. Trybala, V. M. Starov, *Colloids Interfaces* **2018**, *2*, 56.
- [166] *Colloidal Particles at Liquid Interfaces*, (Eds: B. P. Binks, T. S. Horozov), Cambridge University Press, Cambridge **2006**.
- [167] S. Lam, K. P. Velikov, O. D. Velev, *Curr. Opin. Colloid Interface Sci.* **2014**, *19*, 490.
- [168] D. Gonzalez Ortiz, C. Pochat-Bohatier, J. Cambedouzou, M. Bechelany, P. Miele, *Engineering* **2020**, *6*, 468.
- [169] P. F. Marina, J. Xu, X. Wu, H. Xu, *Chem. Sci.* **2018**, *9*, 4821.
- [170] K. G. Marinova, R. G. Alargova, N. D. Denkov, O. D. Velev, D. N. Petsev, I. B. Ivanov, R. P. Borwankar, *Langmuir* **1996**, *12*, 2045.
- [171] P. Creux, J. Lachaise, A. Graciaa, J. K. Beattie, A. M. Djerdjev, *J. Phys. Chem. B* **2009**, *113*, 14146.
- [172] J. K. Beattie, A. M. Djerdjev, *Angew. Chem. Int. Ed.* **2004**, *43*, 3568.
- [173] C. Tang, Y. Chen, J. Luo, M. Y. Low, Z. Shi, J. Tang, Z. Zhang, B. Peng, K. C. Tam, *Cellulose* **2019**, *26*, 7753.
- [174] L. Bai, S. Huan, B. Zhao, Y. Zhu, J. Esquena, F. Chen, G. Gao, E. Zussman, G. Chu, O. J. Rojas, *ACS Nano* **2020**, *14*, 13380.
- [175] P. Bertsch, M. Diener, J. Adamcik, N. Scheuble, T. Geue, R. Mezzenga, P. Fischer, *Langmuir* **2018**, *34*, 15195.
- [176] J. Ojala, J. A. Sirviö, H. Liimatainen, *Chem. Eng. J.* **2016**, *288*, 312.
- [177] M. M. González, C. Blanco-Tirado, M. Y. Combariza, *Fuel* **2020**, *264*, 116830.
- [178] I. Kalashnikova, H. Bizot, B. Cathala, I. Capron, *Langmuir* **2011**, *27*, 7471.
- [179] I. Kalashnikova, H. Bizot, B. Cathala, I. Capron, *Biomacromolecules* **2012**, *13*, 267.
- [180] M. Fathi, M. Vinceković, S. Jurić, M. Viskić, A. Režek Jamrak, F. Donsi, *Food Rev. Int.* **2021**, *37*, 1.
- [181] A. Ahmed, I. Hassan, A. S. Helal, V. Sencadas, A. Radhi, C. K. Jeong, M. F. El-Kady, *iScience* **2020**, *23*, 101286.
- [182] X. Chen, Z. Ren, M. Han, J. Wan, H. Zhang, *Nano Energy* **2020**, *75*, 104980.
- [183] L. Huang, S. Lin, Z. Xu, H. Zhou, J. Duan, B. Hu, J. Zhou, *Adv. Mater.* **2020**, *32*, 1902034.
- [184] E. Fukada, *J. Phys. Soc. Jpn.* **1955**, *10*, 149.
- [185] L. Csoka, I. C. Hoeger, O. J. Rojas, I. Peszlen, J. J. Pawlak, P. N. Peralta, *ACS Macro Lett.* **2012**, *1*, 867.
- [186] A. Hänninen, E. Sarlin, I. Lyyra, T. Salpavaara, M. Kellomäki, S. Tuukkanen, *Carbohydr. Polym.* **2018**, *202*, 418.
- [187] S. Rajala, T. Siponkoski, E. Sarlin, M. Mettänen, M. Vuoriluoto, A. Pammo, J. Juuti, O. J. Rojas, S. Franssila, S. Tuukkanen, *ACS Appl. Mater. Interfaces* **2016**, *8*, 15607.
- [188] Q. Zheng, H. Zhang, H. Mi, Z. Cai, Z. Ma, S. Gong, *Nano Energy* **2016**, *26*, 504.
- [189] F. Ram, A. Gudadhe, T. Vijayakanth, S. Aherrao, V. Borkar, R. Boomishankar, K. Shanmuganathan, *ACS Appl. Polym. Mater.* **2020**, *2*, 2550.
- [190] S. Moheimani, A. Fleming, *Piezoelectric Transducers for Vibration Control and Damping*, Advances in Industrial Control, Springer, London **2006**, tex.lccn: 2006921994.
- [191] W.-S. Jung, M.-G. Kang, H. G. Moon, S.-H. Baek, S.-J. Yoon, Z.-L. Wang, S.-W. Kim, C.-Y. Kang, *Sci. Rep.* **2015**, *5*, 9309.
- [192] X. Chen, Y. Song, Z. Su, H. Chen, X. Cheng, J. Zhang, M. Han, H. Zhang, *Nano Energy* **2017**, *38*, 43.
- [193] S. Chandrasekaran, C. Bowen, J. Roscow, Y. Zhang, D. K. Dang, E. J. Kim, R. D. K. Misra, L. Deng, J. S. Chung, S. H. Hur, *Phys. Rep.* **2019**, *792*, 1.
- [194] H.-J. Kim, E.-C. Yim, J.-H. Kim, S.-J. Kim, J.-Y. Park, I.-K. Oh, *Nano Energy* **2017**, *33*, 130.
- [195] Y. García, Y. B. Ruiz-Blanco, Y. Marrero-Ponce, C. M. Sotomayor-Torres, *Sci. Rep.* **2016**, *6*, 34616.
- [196] K. A. Werling, G. R. Hutchison, D. S. Lambrecht, *J. Phys. Chem. Lett.* **2013**, *4*, 1365.
- [197] B. Frka-Petesic, B. Jean, L. Heux, *EPL* **2014**, *107*, 28006.
- [198] I. Chae, C. K. Jeong, Z. Ounaies, S. H. Kim, *ACS Appl. Bio Mater.* **2018**, *1*, 936.
- [199] J. P. F. Lagerwall, C. Schütz, M. Salajkova, J. Noh, J. Hyun Park, G. Scalia, L. Bergström, *NPG Asia Mater* **2014**, *6*, e80.
- [200] A. Cuetos, M. Dijkstra, *Phys. Rev. Lett.* **2007**, *98*, 095701.
- [201] S. Dussi, M. Dijkstra, *Nat Commun* **2016**, *7*, 11175.
- [202] L. Onsager, *Ann. New York Acad. Sci.* **1949**, *51*, 627.
- [203] K. W. Klockars, B. L. Tardy, M. Borghei, A. Tripathi, L. G. Greca, O. J. Rojas, *Biomacromolecules* **2018**, *19*, 2931.
- [204] A. G. Dumanli, H. M. van der Kooij, G. Kamita, E. Reisner, J. J. Baumberg, U. Steiner, S. Vignolini, *ACS Appl. Mater. Interfaces* **2014**, *6*, 12302.
- [205] Y. Li, J. Jun-Yan Suen, E. Prince, E. M. Larin, A. Klinkova, H. Thérien-Aubin, S. Zhu, B. Yang, A. S. Helmy, O. D. Lavrentovich, E. Kumacheva, *Nat. Commun.* **2016**, *7*, 12520.
- [206] P.-X. Wang, W. Y. Hamad, M. J. MacLachlan, *Nat. Commun.* **2016**, *7*, 11515.
- [207] Z. Wang, Y. Yuan, J. Hu, J. Yang, F. Feng, Y. Yu, P. Liu, Y. Men, J. Zhang, *Carbohydr. Polym.* **2020**, *245*, 116459.
- [208] Z. Wang, N. Li, L. Zong, J. Zhang, *Curr. Opin. Solid State Mater. Sci.* **2019**, *23*, 142.
- [209] Q. Chen, P. Liu, F. Nan, L. Zhou, J. Zhang, *Biomacromolecules* **2014**, *15*, 4343.
- [210] A. Bishopp, M. J. Bennett, *Nature* **2015**, *517*, 558.
- [211] J. J. Lyczakowski, M. Bourdon, O. M. Terrett, Y. Helariutta, R. Wightman, P. Dupree, *Front. Plant Sci.* **2019**, *10*, 1398.

- [212] J. Zhang, Y. S. Choi, C. G. Yoo, T. H. Kim, R. C. Brown, B. H. Shanks, *ACS Sustainable Chem. Eng.* **2015**, 3, 293.
- [213] O. M. Terrett, J. J. Lyczakowski, L. Yu, D. Iuga, W. T. Franks, S. P. Brown, R. Dupree, P. Dupree, *Nat Commun* **2019**, 10, 4978.
- [214] M. Zhu, C. Jia, Y. Wang, Z. Fang, J. Dai, L. Xu, D. Huang, J. Wu, Y. Li, J. Song, Y. Yao, E. Hitz, Y. Wang, L. Hu, *ACS Appl. Mater. Interfaces* **2018**, 10, 28566.
- [215] T. Li, J. Song, X. Zhao, Z. Yang, G. Pastel, S. Xu, C. Jia, J. Dai, C. Chen, A. Gong, F. Jiang, Y. Yao, T. Fan, B. Yang, L. Wågberg, R. Yang, L. Hu, *Sci. Adv.* **2018**, 4, eaar3724.
- [216] J. Song, C. Chen, S. Zhu, M. Zhu, J. Dai, U. Ray, Y. Li, Y. Kuang, Y. Li, N. Quispe, Y. Yao, A. Gong, U. H. Leiste, H. A. Bruck, J. Y. Zhu, A. Vellore, H. Li, M. L. Minus, Z. Jia, A. Martini, T. Li, L. Hu, *Nature* **2018**, 554, 224.
- [217] M. Zhu, Y. Wang, S. Zhu, L. Xu, C. Jia, J. Dai, J. Song, Y. Yao, Y. Wang, Y. Li, D. Henderson, W. Luo, H. Li, M. L. Minus, T. Li, L. Hu, *Adv. Mater.* **2017**, 29, 1606284.
- [218] C. Jia, T. Li, C. Chen, J. Dai, I. M. Kierzewski, J. Song, Y. Li, C. Yang, C. Wang, L. Hu, *Nano Energy* **2017**, 36, 366.
- [219] T. Zhou, J.-W. Wang, M. Huang, R. An, H. Tan, H. Wei, Z.-D. Chen, X. Wang, X. Liu, F. Wang, J. He, *Small* **2019**, 15, 1901079.
- [220] Q. Fu, Y. Chen, M. Sorieul, *ACS Nano* **2020**, 14, 3528.
- [221] T. Li, S. X. Li, W. Kong, C. Chen, E. Hitz, C. Jia, J. Dai, X. Zhang, R. Briber, Z. Siwy, M. Reed, L. Hu, *Sci. Adv.* **2019**, 5, eaau4238.
- [222] D. Hou, T. Li, X. Chen, S. He, J. Dai, S. A. Mofid, D. Hou, A. Iddya, D. Jassby, R. Yang, L. Hu, Z. J. Ren, *Sci. Adv.* **2019**, 5, eaaw3203.
- [223] F. Chen, A. S. Gong, M. Zhu, G. Chen, S. D. Lacey, F. Jiang, Y. Li, Y. Wang, J. Dai, Y. Yao, J. Song, B. Liu, K. Fu, S. Das, L. Hu, *ACS Nano* **2017**, 11, 4275.
- [224] R. L. Pereira Oliveira Moreira, J. A. Simão, R. F. Gouveia, M. Strauss, *ACS Appl. Bio Mater.* **2020**, 3, 2193.
- [225] R. Merindol, S. Diabang, R. Mujica, V. Le Houerou, T. Roland, C. Gauthier, G. Decher, O. Felix, *ACS Nano* **2020**, 14, 16525.
- [226] D. Novel, S. Ghio, A. Gaiardo, A. Picciotto, V. Guidi, G. Speranza, M. Boscardin, P. Bellutti, N. M. Pugno, *Nanomaterials* **2020**, 10, 478.



Paolo Bettotti is a professor in the Department of Physics at the University of Trento. He pursued both fundamental and applied research on silicon nanostructured materials (silicon QDs, photonic crystals, optical sensors, photovoltaics) and integrated silicon photonics. His current research interests span over nanocellulose functional materials and silicon-based neuromorphic photonics.



Marina Scarpa is currently a Full Professor of Biophysics in the Department of Physics at the University of Trento. After the Master Degree in Chemistry, she received a Ph.D. in Molecular Biology from the University of Padova in 1987. Her main research focused on the use of biophysical tools, such as fluorescence and magnetic resonance spectroscopy, electrochemistry, microfluidics, and biosensing for the study of the reactivity of biological macromolecules and their interaction with surfaces. Recently, she expanded her interest toward the nanostructures of biological source and their composites to obtain functional materials.